REPORT ON A HELICOPTER-BORNE

VERSATILE TIME DOMAIN ELECTROMAGNETIC (VTEM^plus) AND

AEROMAGNETIC GEOPHYSICAL SURVEY

Daguilar, Moores & WartHill Blocks

Strathgordon, Tasmania, Australia

For:

Frontier Resources Ltd.

By:

Geotech Ltd.

245 Industrial Parkway North

Aurora, ON, CANADA, L4G 4C4

Tel: 1.905.841.5004

Fax: 1.905.841.0611

www.geotech.ca

Email: info@geotech.ca

Survey flown during February 2012

Project AA926

March 2012

TABLE OF CONTENTS

REPORT ON A HELICOPTER-BORNE
VERSATILE TIME DOMAIN ELECTROMAGNETIC (VTEM^plus) and
AEROMAGNETIC SURVEY

Daguliar, Moores and WartHill Blocks
Strathgordon, Tasmania

EXECUTIVE SUMMARY

During February 1st to 23rd 2012 Geotech Airborne Pty Ltd. carried out a helicopter-borne geophysical survey over the Daguilar, Moores and WartHill Blocks situated approximately 33 kilometres west of Strathgordon, Tasmania.

Principal geophysical sensors included a versatile time domain electromagnetic (VTEM^plus) system, and a caesium magnetometer. Ancillary equipment included a GPS navigation system and a radar altimeter. A total of 955 line-kilometres of geophysical data were acquired during the survey.

In-field data quality assurance and preliminary processing were carried out on a daily basis during the acquisition phase. Preliminary and final data processing, including generation of final digital data and map products were undertaken from the office of Geotech Ltd. in Aurora, Ontario.

The processed survey results are presented as the following maps:

- Electromagnetic stacked profiles of the B-field Z Component,
- Electromagnetic stacked profiles of dB/dt Z Components,
- Colour grids of a B-Field Z Component Channel,
- Total Magnetic Intensity (TMI), and
- EM Time-constant dB/dt Z Component (Tau), are presented.

Digital data includes all electromagnetic and magnetic products, plus ancillary data including the waveform.

The survey report describes the procedures for data acquisition, processing, final image presentation and the specifications for the digital data set.

1. INTRODUCTION

1.1 General Considerations

Geotech Airborne Pty Ltd. performed a helicopter-borne geophysical survey over the Daguliar, Moores and WartHill Blocks situated approximately 33 kilometres west of Strathgordon, Tasmania (Figure 1 & Figure 2).

Grant Macdonald represented Frontier Resources Ltd. during the data acquisition and data processing phases of this project.

The geophysical surveys consisted of helicopter borne EM using the versatile time-domain electromagnetic (VTEM plus) system with Z and X component measurements and aeromagnetics using a caesium magnetometer. A total of 955 line-km of geophysical data were acquired during the survey.

The crew was based out of Lake Pedder Lodge (Figure 2) in Strathgordon, Tasmania for the acquisition phase of the survey. Survey flying started on February 1st 2012 and was completed on February 23rd 2012.

Data quality control and quality assurance, and preliminary data processing were carried out on a daily basis during the acquisition phase of the project. Final data processing followed immediately after the end of the survey. Final reporting, data presentation and archiving were completed from the Aurora office of Geotech Ltd. in March and April, 2012.
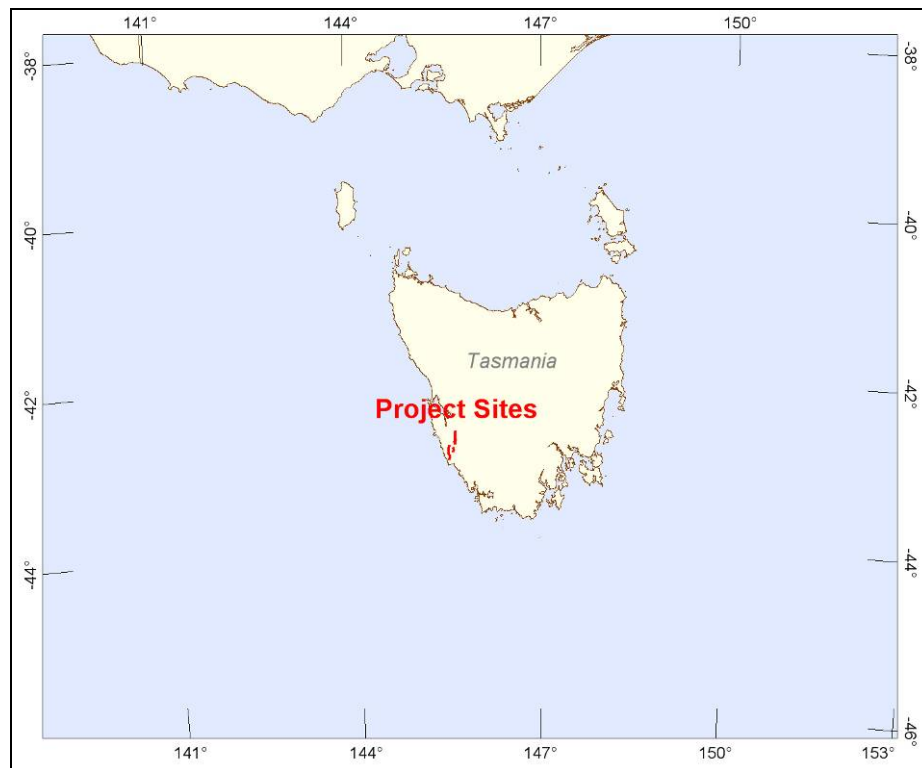
Figure 1: Property Location

1.2 Survey and System Specifications

The Daguilar, Moores and WartHill Blocks are located approximately 33 km west of Strathgordon, Tasmania, Australia (Figure 2).

Figure 2: Survey areas location on Google Earth

The all the survey blocks were flown in an east to west (N 90° E azimuth) direction, with traverse line spacing of 150 metres as depicted in Figure 3. Tie lines were flown perpendicular to the traverse lines (N 0° E azimuth) at a spacing of 1400/1500 metres respectively. For more detailed information on the flight spacing and direction see Table 1.

1.3   Topographic Relief and Cultural Features

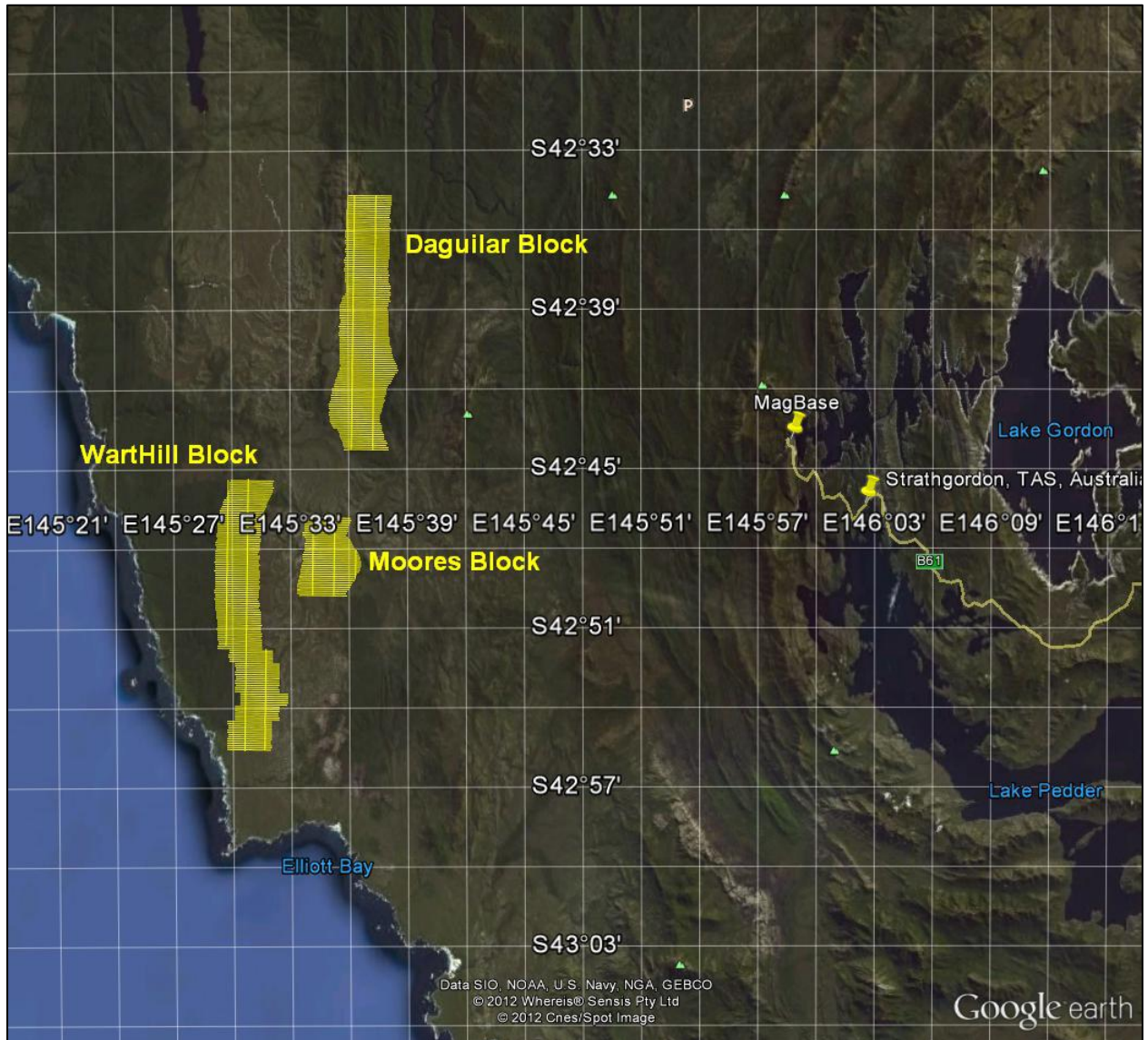Topographically, the Daguilar, Moores and WartHill Blocks exhibits a shallow relief with an elevation ranging from 23 to 723 metres above mean sea level over an area of 135 square kilometres (Figure 3).

The survey block has various rivers and streams running through the survey area which connect various lakesThere are a few visible signs of culture such as roads located throughout the survey areas.
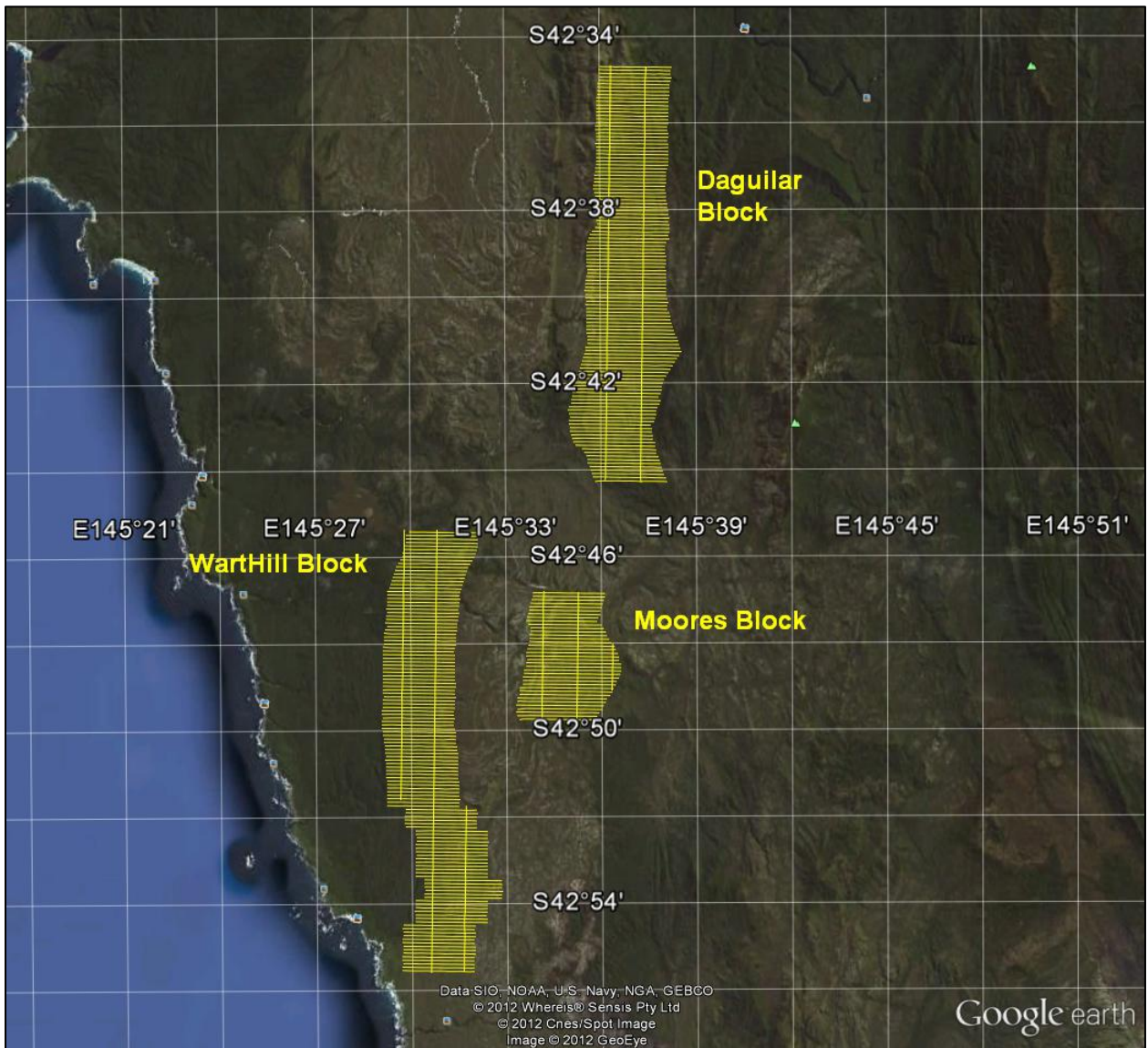

Figure 3: Flight paths over a Google Earth Image

.

2.   DATA ACQUISITION

2.1   Survey Area

The survey block (see Figure 3 and Appendix A) and general flight specifications are as follows:

Table 1: Survey Specifications

Survey block	Traverse Line spacing (m)	Area (Km^2)	Planned[1] Line-km	Actual Line-km	Flight direction	Line numbers
Daguilar	Traverse: 150	59	403	403.2	N 90° E / N 270° E	L10010 – L11190
	Tie: 1500			35.6	N 0° E / N 180° E	T91010 – T91020
Moores	Traverse: 150	18	135	133.1	N 90° E / N 270° E	L30010 – L30370
	Tie: 1500			13	N 0° E / N 180° E	T93010 – T93030
WartHill	Traverse: 150	58	417	392.1	N 90° E / N 270° E	L20010 – L21260
	Tie: 1400			37.6	N 0° E / N 180° E	T92010– T92030
TOTAL		135	955	1014.6		

Survey block boundaries co-ordinates are provided in Appendix B.

2.2   Survey Operations

Survey operations were based out of Strathgordon, Tasmania from February 1st to February 23rd 2012. The following table shows the timing of the flying.

Table 2: Survey schedule

Date	Flight #	Flow km	Block	Crew location	Comments
1-Feb-2012				Strathgordon, Tasmania	Crew mobilized
2-Feb-2012				Strathgordon, Tasmania	Crew mobilized
3-Feb-2012				Strathgordon, Tasmania	Crew mobilized
4-Feb-2012				Strathgordon, Tasmania	Crew mobilized
5-Feb-2012				Strathgordon, Tasmania	Crew mobilized
6-Feb-2012				Strathgordon, Tasmania	System assembly
7-Feb-2012				Strathgordon, Tasmania	System assembly
8-Feb-2012				Strathgordon, Tasmania	System assembly
9-Feb-2012				Strathgordon, Tasmania	System assembly
10-Feb-2012	1			Strathgordon, Tasmania	Test flight
11-Feb-2012	2,3			Strathgordon, Tasmania	Test flights
12-Feb-2012	4	78	warthill	Strathgordon, Tasmania	78km flown limited production due to fuel
13-Feb-2012				Strathgordon, Tasmania	No production due to weather
14-Feb-2012	5,6,7	261	Daguilar/ moores	Strathgordon, Tasmania	261 km flown
15-Feb-2012	8,9,10	280	Daguilar/ moores	Strathgordon, Tasmania	280km flown

---

[1] Note: Actual Line kilometres represent the total line kilometres in the final database. These line-km normally exceed the Planned line-km, as indicated in the survey NAV files.

Date	Flight #	Flow km	Block	Crew location	Comments
16-Feb-2012				Strathgordon, Tasmania	No production due to weather
17-Feb-2012				Strathgordon, Tasmania	No production due to weather
18-Feb-2012	11,12,13	301	Daguilar/ moores/ warthill	Strathgordon, Tasmania	301km flown
19-Feb-2012				Strathgordon, Tasmania	No production due to weather
20-Feb-2012				Strathgordon, Tasmania	No production due to weather
21-Feb-2012				Strathgordon, Tasmania	No production due to weather
22-Feb-2012	14,15	146	Warthill/ moores	Strathgordon, Tasmania	146km flown
23-Feb-2012				Strathgordon, Tasmania	

2.3 Flight Specifications

During the survey the helicopter was maintained at a mean altitude of 79 metres above the ground with an average survey speed of 80 km/hour. This allowed for an actual average EM bird terrain clearance of 43 metres and a magnetic sensor clearance of 66 metres.

The on board operator was responsible for monitoring the system integrity. He also maintained a detailed flight log during the survey, tracking the times of the flight as well as any unusual geophysical or topographic features.

On return of the aircrew to the base camp the survey data was transferred from a compact flash card (PCMCIA) to the data processing computer. The data were then uploaded via ftp to the Geotech office in Aurora for daily quality assurance and quality control by qualified personnel.

2.4 Aircraft and Equipment

2.4.1 Survey Aircraft

The survey was flown using a Eurocopter Aerospatiale (Astar) 350 B3 helicopter, registration VH-VTN. The helicopter is owned and operated by United Aero Helicopters. Installation of the geophysical and ancillary equipment was carried out by a Geotech Ltd crew.

2.4.2 Electromagnetic System

The electromagnetic system was a Geotech Time Domain EM (VTEM^{plus}) system. VTEM, with the serial number 12 had been used for the survey. The configuration is as indicated in Figure 5.

The VTEM^{plus} Receiver and transmitter coils were in concentric-coplanar and Z-direction oriented configuration. The receiver system for the project also included a coincident-coaxial X-direction coil to measure the in-line dB/dt and calculate B-Field responses. The EM bird was towed at a mean distance of 35 metres below the aircraft as shown in Figure 5 and Figure 6. The receiver decay recording scheme is shown in
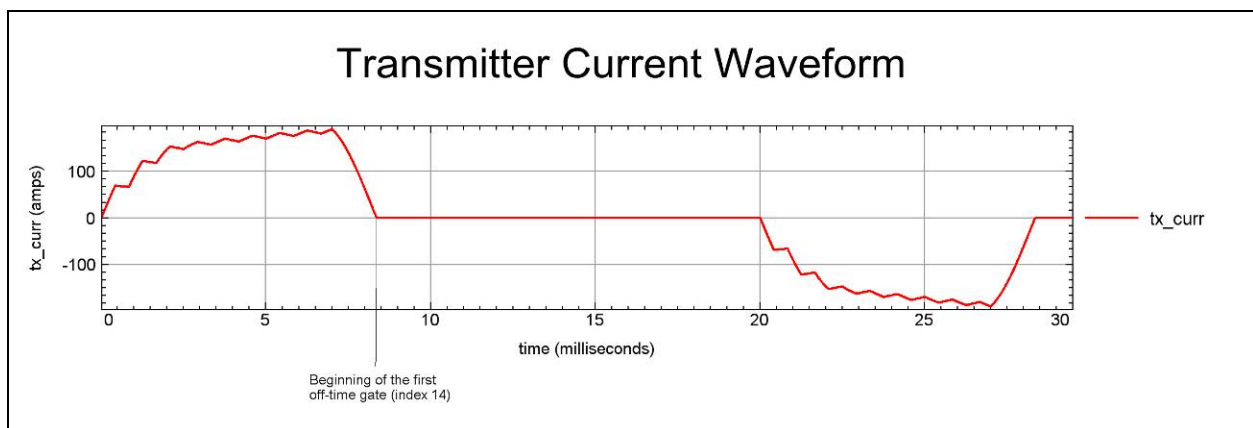.

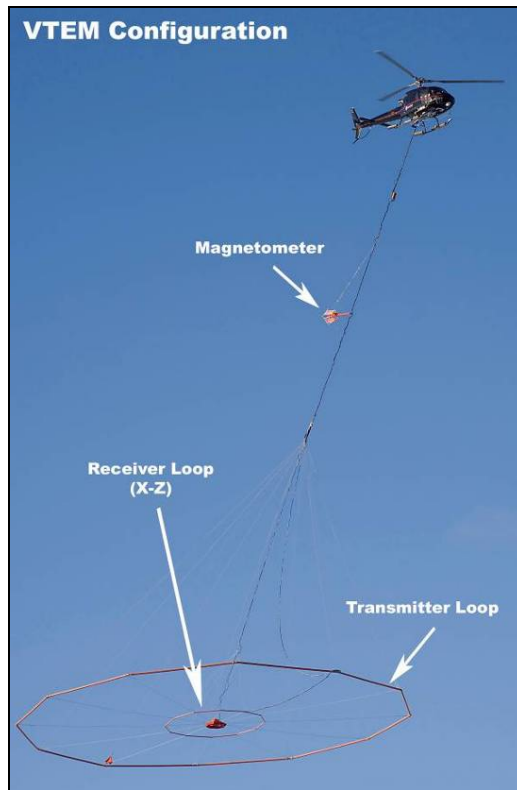**Figure 4:** VTEM Waveform & Sample Times

Figure 5: VTEM^{plus} Configuration, with magnetometer.

The VTEM decay sampling scheme is shown in Table 3 below. Thirty-five time measurement gates were used for the final data processing in the range from 0.083 to 9.286 μ sec.

Table 3: Off-Time Decay Sampling Scheme

VTEM Decay Sampling Scheme			
Index	**Middle**	**Start**	**End**
Milliseconds			
13	0.083	0.078	0.090
14	0.096	0.090	0.103
15	0.110	0.103	0.118
16	0.126	0.118	0.136
17	0.145	0.136	0.156
18	0.167	0.156	0.179
19	0.192	0.179	0.206
20	0.220	0.206	0.236
21	0.253	0.236	0.271
22	0.290	0.271	0.312
23	0.333	0.312	0.358
24	0.383	0.358	0.411
25	0.440	0.411	0.472
26	0.505	0.472	0.543
27	0.580	0.543	0.623
28	0.667	0.623	0.716
29	0.766	0.716	0.823
30	0.880	0.823	0.945
31	1.010	0.945	1.086
32	1.161	1.086	1.247
33	1.333	1.247	1.432
34	1.531	1.432	1.646
35	1.760	1.646	1.891
36	2.021	1.891	2.172
37	2.323	2.172	2.495
38	2.667	2.495	2.865
39	3.063	2.865	3.292
40	3.521	3.292	3.781
41	4.042	3.781	4.341
42	4.641	4.341	4.987
43	5.333	4.987	5.729
44	6.125	5.729	6.581
45	7.036	6.581	7.560
46	8.083	7.560	8.685
47	9.286	8.685	9.977

Z Component: 13-47 time gates
X Component: 20-47 time gates.

VTEM^plus system specification:

- Transmitter loop diameter: 26 m
- Effective coil area: 2123 m^2
- Number of turns: 4
- Transmitter base frequency: 25 Hz
- Peak current: 189 A
- Pulse width: 8.37 ms
- Wave form shape: trapezoid
- Peak dipole moment: 401,382 nIA
- Actual average EM Bird terrain clearance: 43 metres above the ground

Receiver

- X Coil diameter: 0.32 m
- Number of turns: 245
- Effective coil area: 19.69 m^2
- Z-Coil coil diameter: 1.2 m
- Number of turns: 100
- Effective coil area: 113.04 m^2
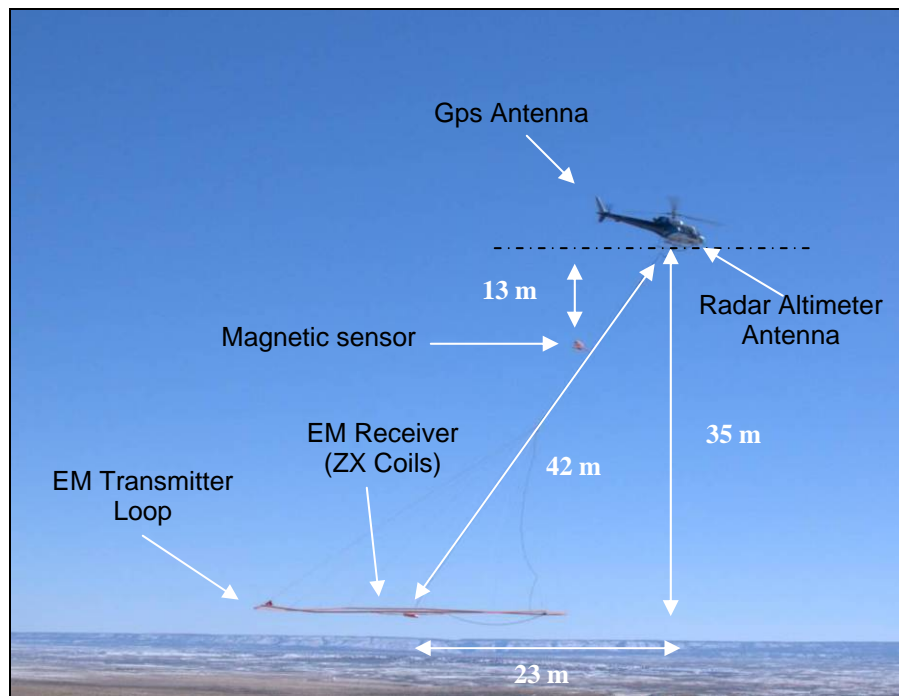
Figure 6: VTEM^plus System Configuration

2.4.3 Airborne magnetometer

The magnetic sensor utilized for the survey was Geometrics optically pumped caesium vapour magnetic field sensor mounted 13 metres below the helicopter, as shown in Figure 6. The sensitivity of the magnetic sensor is 0.02 nanoTesla (nT) at a sampling interval of 0.1 seconds.

2.4.4 Radar Altimeter

A Terra TRA 3000/TRI 40 radar altimeter was used to record terrain clearance. The antenna was mounted beneath the bubble of the helicopter cockpit (Figure 6).

2.4.5 GPS Navigation System

The navigation system used was a Geotech PC104 based navigation system utilizing a NovAtel's WAAS (Wide Area Augmentation System) enable OEM4-G2-3151W GPS receiver, Geotech navigate software, a full screen display with controls in front of the pilot to direct the flight and an NovAtel GPS antenna mounted on the helicopter tail (Figure 6). As many as 11 GPS and two WAAS satellites may be monitored at any one time. The positional accuracy or circular error probability (CEP) is 1.8 m, with WAAS active, it is 1.0 m. The co-ordinates of the block were set-up prior to the survey and the information was fed into the airborne navigation system.

2.4.6 Digital Acquisition System

A Geotech data acquisition system recorded the digital survey data on an internal compact flash card. Data is displayed on an LCD screen as traces to allow the operator to monitor the integrity of the system. The data type and sampling interval as provided in Table 4.

Table 4: Acquisition Sampling Rates

Data Type	Sampling
TDEM	0.1 sec
Magnetometer	0.1 sec
GPS Position	0.2 sec
Radar Altimeter	0.2 sec

2.5   Base Station

A combined magnetometer/GPS base station was utilized on this project. A Geometrics Caesium vapour magnetometer was used as a magnetic sensor with a sensitivity of 0.001 nT. The base station was recording the magnetic field together with the GPS time at 1 Hz on a base station computer.

The base station magnetometer sensor was installed at a secute location adjacent to landing pad (42°43'56."S, 53°145'58.42"E); away from electric transmission lines and moving ferrous objects such as motor vehicles. The base station data were backed-up to the data processing computer at the end of each survey day.

3. PERSONNEL

The following Geotech Ltd. personnel were involved in the project.

Field:

Project Manager:	Adam Ellis (Office)
Data QC:	Peter Holbrook (Office)
Crew chief:	Leon Lovelock
Operator:	Jon Lambert

The survey pilot and the mechanical engineer were employed directly by the helicopter operator – United Aero Helicopters.

Pilot:	Colby Tyrrell
Mechanical Engineer:	n/a

Office:

Preliminary Data Processing:	Peter Helbrook
Final Data Processing:	Keeme Mokubung
Final Data QA/QC:	Alexander Prikhodko
Reporting/Mapping:	Corrie Laver

Data acquisition phase was carried out under the supervision of Andrei Bagrianski, P. Geo, Chief Operating Officer. The processing and interpretation phase was under the supervision of Alexander Prikhodko, P. Geo. The customer relations were looked after by Keith Fisk.

4. DATA PROCESSING AND PRESENTATION

Data compilation and processing were carried out by the application of Geosoft OASIS Montaj and programs proprietary to Geotech Ltd.

4.1 Flight Path

The flight path, recorded by the acquisition program as WGS 84 latitude/longitude, was converted into the GDA94, UTM Zone 55 South coordinate system in Oasis Montaj.

The flight path was drawn using linear interpolation between x, y positions from the navigation system. Positions are updated every second and expressed as UTM easting's (x) and UTM northing's (y).

4.2 Electromagnetic Data

A three stage digital filtering process was used to reject major sferic events and to reduce system noise. Local sferic activity can produce sharp, large amplitude events that cannot be removed by conventional filtering procedures. Smoothing or stacking will reduce their amplitude but leave a broader residual response that can be confused with geological phenomena. To avoid this possibility, a computer algorithm searches out and rejects the major sferic events.

The signal to noise ratio was further improved by the application of a low pass linear digital filter. This filter has zero phase shift which prevents any lag or peak displacement from occurring, and it suppresses only variations with a wavelength less than about 1 second or 15 metres. This filter is a symmetrical 1 sec linear filter.

The results are presented as stacked profiles of EM voltages for the time gates, in linear - logarithmic scale for the B-field Z component and dB/dt responses in the Z and X components. B-field Z component time channel recorded at 2.021 and 0.880 milliseconds after the termination of the impulse is also presented as contour colour images. Fraser Filter X component is also presented as a colour image. Calculated Time Constant (TAU) with anomaly contours of Calculated Vertical Derivative of TMI is presented in Appendix C and E. Resistivity Depth Image (RDI) is also presented in Appendix C and F.

VTEM plus has two receiver coil orientations. Z-axis coil is oriented parallel to the transmitter coil axis and both are horizontal to the ground. The X-axis coil is oriented parallel to the ground and along the line-of-flight. This combined two coil configuration provides information on the position, depth, dip and thickness of a conductor. Generalized modeling results of VTEM plus data are shown in Appendix D.

In general X-component data produce cross-over type anomalies: from "+ to – "in flight direction of flight for "thin" sub vertical targets and from "- to +" in direction of flight for "thick" targets. Z component data produce double peak type anomalies for "thin" sub vertical targets and single peak for "thick" targets.

The limits and change-over of "thin-thick" depends on dimensions of a TEM system.

Because of X component polarity is under line-of-flight, convolution Fraser filter (FF, Figure 7) is applied to X component data to represent axes of conductors in the form of

grid map. In this case positive FF anomalies always correspond to "plus-to-minus" X data crossovers independently of direction of flight.
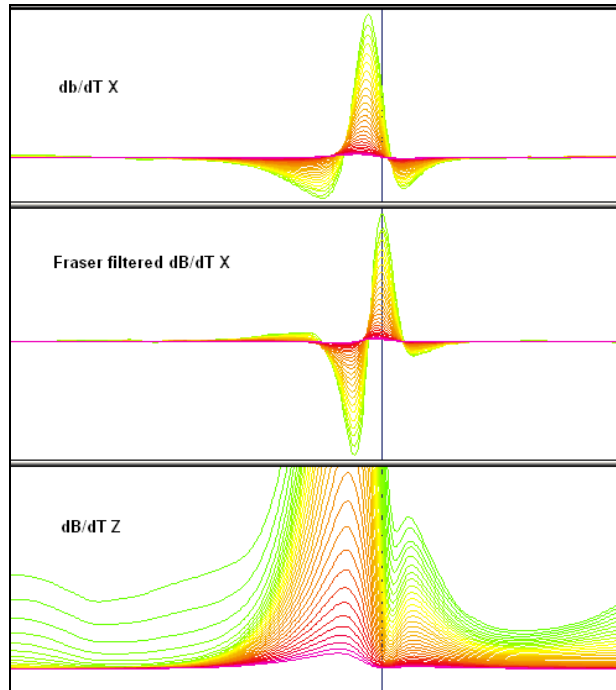

Figure 7: Z, X and Fraser filtered X (FFx) components for "thin" target

4.3   Magnetic Data

The processing of the magnetic data involved the correction for diurnal variations by using the digitally recorded ground base station magnetic values. The base station magnetometer data was edited and merged into the Geosoft GDB database on a daily basis. The aeromagnetic data was corrected for diurnal variations by subtracting the observed magnetic base station deviations.

Tie line levelling was carried out by adjusting intersection points along traverse lines. A micro-levelling procedure was applied to remove persistent low-amplitude components of flight-line noise remaining in the data.

The corrected magnetic data was interpolated between survey lines using a random point gridding method to yield x-y grid values for a standard grid cell size of approximately 37.5 metres at the mapping scale. The Minimum Curvature algorithm was used to interpolate values onto a rectangular regular spaced grid.

5.   DELIVERABLES

5.1   Survey Report

The survey report describes the data acquisition, processing, and final presentation of the survey results. The survey report is provided in two paper copies and digitally in PDF format.

5.2   Maps

Final maps were produced at a scale of 1:10,000 for Moores Block & 1:25,000 for Daguilar and Warthill blocks, for best representation of the survey size and line spacing. The coordinate/projection system used was GDA94 Datum, Map Grid of Australia 55 South. All maps show the mining claims, flight path trace and topographic data; latitude and longitude are also noted on maps.

The preliminary and final results of the survey are presented as EM profiles, a late-time gate gridded EM channel, and a color magnetic TMI contour map. The following maps are presented on paper;

- VTEM dB/dt profiles Z Component, Time Gates 0.220 – 7.036 ms in linear – logarithmic scale.
- VTEM B-Field profiles Z Component, Time Gates 0.220 – 7.036 ms in linear – logarithmic scale.
- VTEM B-field late time Z Component colour image.
- VTEM dB/dt Calculated Time Constant (TAU) with contours of anomaly areas of the Calculated Vertical Derivative of TMI
- Reduced to Pole of TMI colour image and contours.

5.3   Digital Data

- Two copies of the data and maps on DVD were prepared to accompany the report. Each DVD contains a digital file of the line data in GDB Geosoft Montaj format as well as the maps in Geosoft Montaj Map and PDF format.

- DVD structure.

> **Data**   contains databases, grids and maps, as described below.
> **Report**   contains a copy of the report and appendices in PDF format.

Databases in Geosoft GDB format, containing the channels listed in Table 5.

Table 5: Geosoft GDB Data Format

Channel name	Units	Description
X_UTM:	metres	UTM Easting WGS84 Zone 55 South
Y_UTM:	metres	UTM Northing WGS84 Zone 55 South
X_MGA:	metres	Map Grid of Australia zone 55 - GDA94
Y_MGA:	metres	Map Grid of Australia zone 55 - GDA94
Z:	metres	GPS antenna elevation (above Geoid)
Longitude:	Decimal Degrees	WGS 84 Longitude data
Latitude:	Decimal Degrees	WGS 84 Latitude data
Radar:	metres	helicopter terrain clearance from radar altimeter
Radarb:	metres	Calculated EM bird terrain clearance from radar altimeter
DEM:	metres	Digital Elevation Model
Gtime:	Seconds of the day	GPS time
Mag1:	nT	Raw Total Magnetic field data
Basemag:	nT	Magnetic diurnal variation data
Mag2:	nT	Diurnal corrected Total Magnetic field data
Mag3:	nT	Levelled Total Magnetic field data
CVG	nT/m	Calculated Vertical Derivative of TMI
RTP	nT	Reduced To Pole of TMI
RTP_CVG	nT/m	Calculated Vertical Derivative of Reduced To Pole of TMI
SFz[13]:	$pV/(A*m^4)$	Z dB/dt 0.083 millisecond time channel
SFz[14]:	$pV/(A*m^4)$	Z dB/dt 0.096 millisecond time channel
SFz[15]:	$pV/(A*m^4)$	Z dB/dt 0.110 millisecond time channel
SFz[16]:	$pV/(A*m^4)$	Z dB/dt 0.126 millisecond time channel
SFz[17]:	$pV/(A*m^4)$	Z dB/dt 0.145 millisecond time channel
SFz[18]:	$pV/(A*m^4)$	Z dB/dt 0.167 millisecond time channel
SFz[19]:	$pV/(A*m^4)$	Z dB/dt 0.192 millisecond time channel
SFz[20]:	$pV/(A*m^4)$	Z dB/dt 0.220 millisecond time channel
SFz[21]:	$pV/(A*m^4)$	Z dB/dt 0.253 millisecond time channel
SFz[22]:	$pV/(A*m^4)$	Z dB/dt 0.290 millisecond time channel
SFz[23]:	$pV/(A*m^4)$	Z dB/dt 0.333 millisecond time channel
SFz[24]:	$pV/(A*m^4)$	Z dB/dt 0.383 millisecond time channel
SFz[25]:	$pV/(A*m^4)$	Z dB/dt 0.440 millisecond time channel
SFz[26]:	$pV/(A*m^4)$	Z dB/dt 0.505 millisecond time channel
SFz[27]:	$pV/(A*m^4)$	Z dB/dt 0.580 millisecond time channel
SFz[28]:	$pV/(A*m^4)$	Z dB/dt 0.667 millisecond time channel
SFz[29]:	$pV/(A*m^4)$	Z dB/dt 0.766 millisecond time channel
SFz[30]:	$pV/(A*m^4)$	Z dB/dt 0.880 millisecond time channel
SFz[31]:	$pV/(A*m^4)$	Z dB/dt 1.010 millisecond time channel
SFz[32]:	$pV/(A*m^4)$	Z dB/dt 1.161 millisecond time channel
SFz[33]:	$pV/(A*m^4)$	Z dB/dt 1.333 millisecond time channel
SFz[34]:	$pV/(A*m^4)$	Z dB/dt 1.531 millisecond time channel
SFz[35]:	$pV/(A*m^4)$	Z dB/dt 1.760 millisecond time channel
SFz[36]:	$pV/(A*m^4)$	Z dB/dt 2.021 millisecond time channel
SFz[37]:	$pV/(A*m^4)$	Z dB/dt 2.323 millisecond time channel
SFz[38]:	$pV/(A*m^4)$	Z dB/dt 2.667 millisecond time channel
SFz[39]:	$pV/(A*m^4)$	Z dB/dt 3.063 millisecond time channel
SFz[40]:	$pV/(A*m^4)$	Z dB/dt 3.521 millisecond time channel
SFz[41]:	$pV/(A*m^4)$	Z dB/dt 4.042 millisecond time channel
SFz[42]:	$pV/(A*m^4)$	Z dB/dt 4.641 millisecond time channel
SFz[43]:	$pV/(A*m^4)$	Z dB/dt 5.333 millisecond time channel
SFz[44]:	$pV/(A*m^4)$	Z dB/dt 6.125 millisecond time channel

Channel name	Units	Description
SFz[45]:	pV/(A*m^4)	Z dB/dt 7.036 millisecond time channel
SFz[46]:	pV/(A*m^4)	Z dB/dt 8.083 millisecond time channel
SFz[47]:	pV/(A*m^4)	Z dB/dt 9.286 millisecond time channel
BFz	(pV*ms)/(A*m4)	Z B-Field data for time channels 14 to 47
NchanBF		Latest time channels of TAU calculation
NchanSF		Latest time channels of TAU calculation
TauBF	milliseconds	Time constant B-Field
TauSF	milliseconds	Time constant dB/dt
PLM		60 Hz power line monitor

Electromagnetic B-field and dB/dt Z component data is found in array channel format between indexes 14 – 45, and X component data from 20 – 45, as described above.

- Database of the VTEM Waveform "AA926_waveform_final.gdb" in Geosoft GDB format, containing the following channels:

  Time: Sampling rate interval, 5.2083 microseconds
  Rx_Volt: Output voltage of the receiver coil (Volt)
  Tx_Current: Output current of the transmitter (Amp)

- Grids in Geosoft GRD format, as follows:

  BFz**:   B-Field Z Component
  Mag3:   Total Magnetic Intensity (nT)
  RTP: Reduced To Pole of TMI (nT)
  CVG_RTP: Calculated Vertical Derivative of TMI (nT/m)
  TauBF: B-Field Calculated Time (ms)
  TauSF: dB/dt Calculated Time Constant (ms)
  SFxFF**:   Fraser Filter X Component dB/dt
  AS: Analytic Signal

  A Geosoft .GRD file has a .GI metadata file associated with it, containing grid projection information. A grid cell size of 37.5 metres was used.

- Maps at 1:10,000 and 1:25,000 in Geosoft MAP format, as follows:

  AA926_*scale*k_dBdtz_*bb*: dB/dt profiles Z Component, Time Gates 0.220 – 7.036 ms in linear – logarithmic scale.
  AA926_*scale*k _Bfield_*bb*: B-field profiles Z Component, Time Gates 0.220 – 7.036 ms in linear – logarithmic scale over total magnetic intensity.
  AA926_*scale*k _BFz_*bb*: B-field late time Z Component color image.
  AA926_*scale*k _SFxFF_*bb*: dB/dt early time X Component Fraser Filter color image.
  AA926_*scale*k _RTP_*bb*: Reduced To Pole of TMI (RTP) color image.
  AA926_*scale*k _TauSF_*bb*: dB/dt Calculated Time Constant (TAU) with contours of anomaly areas of the Calculated Vertical Derivative of TMI
  AA926_*scale*k _AS_*bb*: Analytic Signal

  Where *scale*k represents the scale for that block and *bb* represents the block name.

Maps are also presented in PDF format.

1:50,000 topographic vectors were taken from the NRCAN Geogratis database at;
http://geogratis.gc.ca/geogratis/en/index.html.

- A Google Earth file *AA926_FlightPath.kml* showing the flight path of the block is included. Free versions of Google Earth software from:
http://earth.google.com/download-earth.html

6.   CONCLUSIONS AND RECOMMENDATIONS

A helicopter-borne versatile time domain electromagnetic (VTEM plus) geophysical survey has been completed over the Daguilar, Moores and Warthill Blocks near Strathgordon, Tasmania,

The total area coverage for all properties is 135 km^2. Total survey line coverage is 1014.6 line kilometres. The principal sensors included a Time Domain EM system and a magnetometer. Results have been presented as stacked profiles, and contour color images at a scale of 1:10,000 & 1:25,000.

Daguilar Block

The total area coverage is 59km^2. Total survey line coverage is 438.8 line kilometres.

Based on the geophysical results obtained, the area has several conductive zones. Some of these zones are considered as sub-horizontal lithological conductors, some as steeply dipping structural conductors, and some as local targets (*reference in Appendix C: L10020, L10840 10400 RDI).*

If the conductors correspond to an exploration model on the area it is recommended picking anomalies with conductance grading and center localization of the targets, detail resistivity depth imaging and plate Maxwell modelling for some of the anomalies prior to ground follow up and drill testing are recommended.

WartHill Block

The total area coverage is 58 km^2. Total survey line coverage is 429.7 line kilometres.

Based on the geophysical results obtained, the area has several conductive zones which are considered as gently to steeply dipping structural conductors mostly along the S-N oriented dyke similar magnetic anomalies.

Conductive zone in the SW corner of the block is a linear conductive structure of about 1800m length. The structure is gently dipping to the west, and according to detail resistivity depth section, the top of the EM response is near surface *(reference in Appendix C: L20130 RDI).*

The resistivity depth section for L20520 *(reference in Appendix C: L20520 RDI)* represents a long structural conductor in the centre of the block.

On the northern part of the block there is a broad but linear conductive zone oriented N-S as well. conductive structure is about 5km long and associated with the magnetic anomaly *(reference in Appendix C: L21250 RDI).*
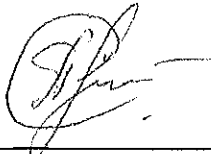
Moores Block

The total area coverage is 18 km^2. Total survey line coverage is 146.1 line kilometres.

Based on the geophysical results obtained, the area consists of conductive zones which are considered as sub-horizontal lithological conductors. Some of them are gently dipping layer-similar conductors (North-East zone), some can be considered as an alteration zone (central part of the block). The local anomaly in the center of the block is crossed by one line (L30150) and must be checked if the anomaly is from man-made source.

(reference in Appendix C: L30150, L30260 & L30350 RDI).
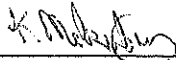
Respectfully submitted[5],

Alexander Prikhodko, P.Geo.
Geotech Ltd.

Peter Holbrook.
Geotech Airborne Pty Ltd.

Keeme Mokubung
Geotech Ltd.

April 2012

[5]Final data processing of the EM and magnetic data were carried out by Keeme Mokubung, from the office of Geotech Ltd. in Aurora, Ontario, under the supervision of Alexander Prikhodko, P.Geo., PhD, Senior Geophysicist, VTEM Interpretation Supervisor.

APPENDIX A

SURVEY BLOCK LOCATION MAP

Survey Overview of the Blocks

APPENDIX B

SURVEY BLOCK COORDINATES

Easting UTM55S	Northing UTM55S
AA926-Daguilar	
385849.2	5267384
387506.5	5267384
387331.2	5268343
387404.2	5269600
387623.3	5270023
387813.2	5270666
387988.4	5271733
388704.2	5272872
388748	5273018
388368.2	5273939
388046.7	5275268
387783.7	5277708
388163.5	5277708
388017.4	5278672
387608.4	5279928
387798.2	5281199
387520.6	5282938
387285.2	5283466
386981.5	5284786
386829.7	5285101
386432.6	5285078
385731.9	5283256
385451.7	5282415
385183.2	5277778
385101.5	5275349
385195	5273270
384412.6	5270420
384412.7	5269848
AA926-Moores	
382344.1	5257166
382299.2	5257795
382859.7	5260691
383793.9	5262607
384401.2	5262607
384424.6	5261392
385872.7	5260528
386316.5	5259734
386316.5	5259080
385264.9	5257166
382344.1	5257166

AA926-WartHill	
377074.8	5253355
376787	5254852
376763.5	5259850
377464.1	5263588
378421.7	5265223
378912.2	5265223
379262.6	5264265
378491.8	5262537
378678.9	5258028
378585.5	5256907
378982.6	5255249
378932.3	5254166
378859	5253369
379326.4	5253369
379326.5	5252361
380305.2	5252347
380305.3	5250360
381327.8	5250360
381327.9	5249352
380349.1	5249352
380320	5248340
379312	5248340
379297.5	5246342
378085	5246342
378106.7	5253355

APPENDIX C

GEOPHYSICAL MAPS[1]
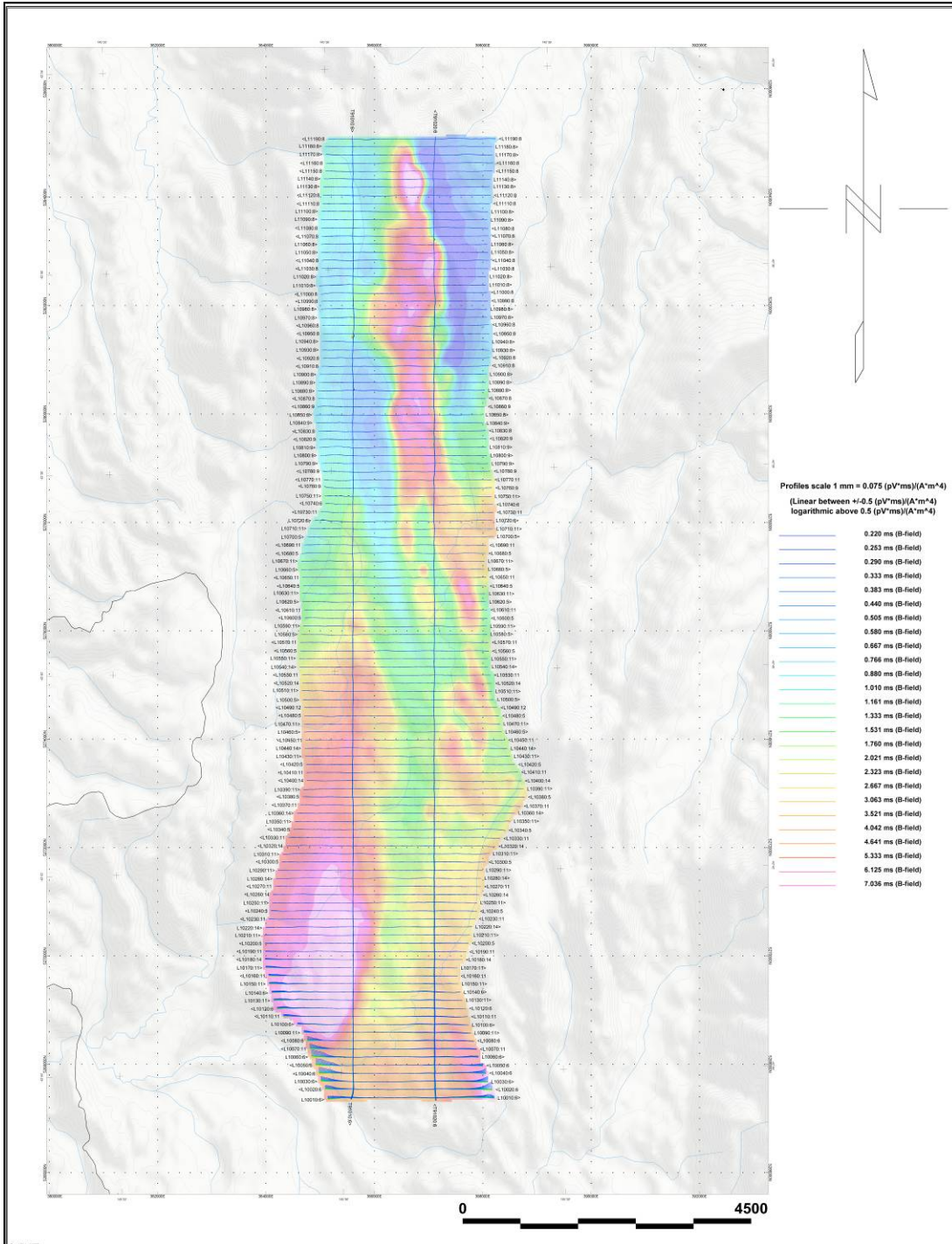
Daguilar Block - VTEM B-Field Z Component Profiles, Time Gates 0.220 to 7.036 ms

---

[1] Full size geophysical maps are also available in PDF format on the final DVD

Daguilar Block - VTEM dB/dt Z Component Profiles, Time Gates 0.220 to 7.036 ms

Profiles scale 1 mm = 0.2 (pV/A*m^4)
Linear between +/-0.5 (pV/A*m^4)
logarithmic above 0.5 (pV/A*m^4)

	0.220 ms
	0.253 ms
	0.290 ms
	0.333 ms
	0.383 ms
	0.440 ms
	0.505 ms
	0.580 ms
	0.667 ms
	0.766 ms
	0.880 ms
	1.010 ms
	1.161 ms
	1.333 ms
	1.531 ms
	1.760 ms
	2.021 ms
	2.323 ms
	2.667 ms
	3.063 ms
	3.521 ms
	4.042 ms
	4.641 ms
	5.333 ms
	6.125 ms
	7.036 ms

0   4500

Daguilar Block - VTEM B-Field Z Component Channel 30, Time Gate 0.880 ms

BFz30
(pV*ms)/(A*m^4)

0.0031	
0.0007	
-0.0004	
-0.0011	
-0.0017	
-0.0020	
-0.0024	
-0.0027	
-0.0029	
-0.0031	
-0.0034	
-0.0036	
-0.0037	
-0.0039	
-0.0041	
-0.0043	
-0.0044	
-0.0046	
-0.0047	
-0.0048	
-0.0050	
-0.0051	
-0.0052	
-0.0054	
-0.0055	
-0.0056	
-0.0058	
-0.0059	
-0.0061	
-0.0062	
-0.0064	
-0.0066	
-0.0068	
-0.0070	
-0.0073	
-0.0077	
-0.0083	
-0.0095	

0   4500

Daguilar Block - dB/dt Calculated Time Constant (Tau) with contours of anomaly areas of the Calculated Vertical Derivative of TMI

Daguilar Block - Reduced to Pole of TMI (RTP)

RTP
(nT)

62223
62180
62153
62137
62126
62116
62106
62095
62089
62084
62079
62076
62073
62070
62067
62064
62062
62060
62057
62055
62054
62052
62049
62047
62045
62043
62040
62038
62035
62032
62030
62028
62025
62023
62020
62016
62012
62005

0   4500
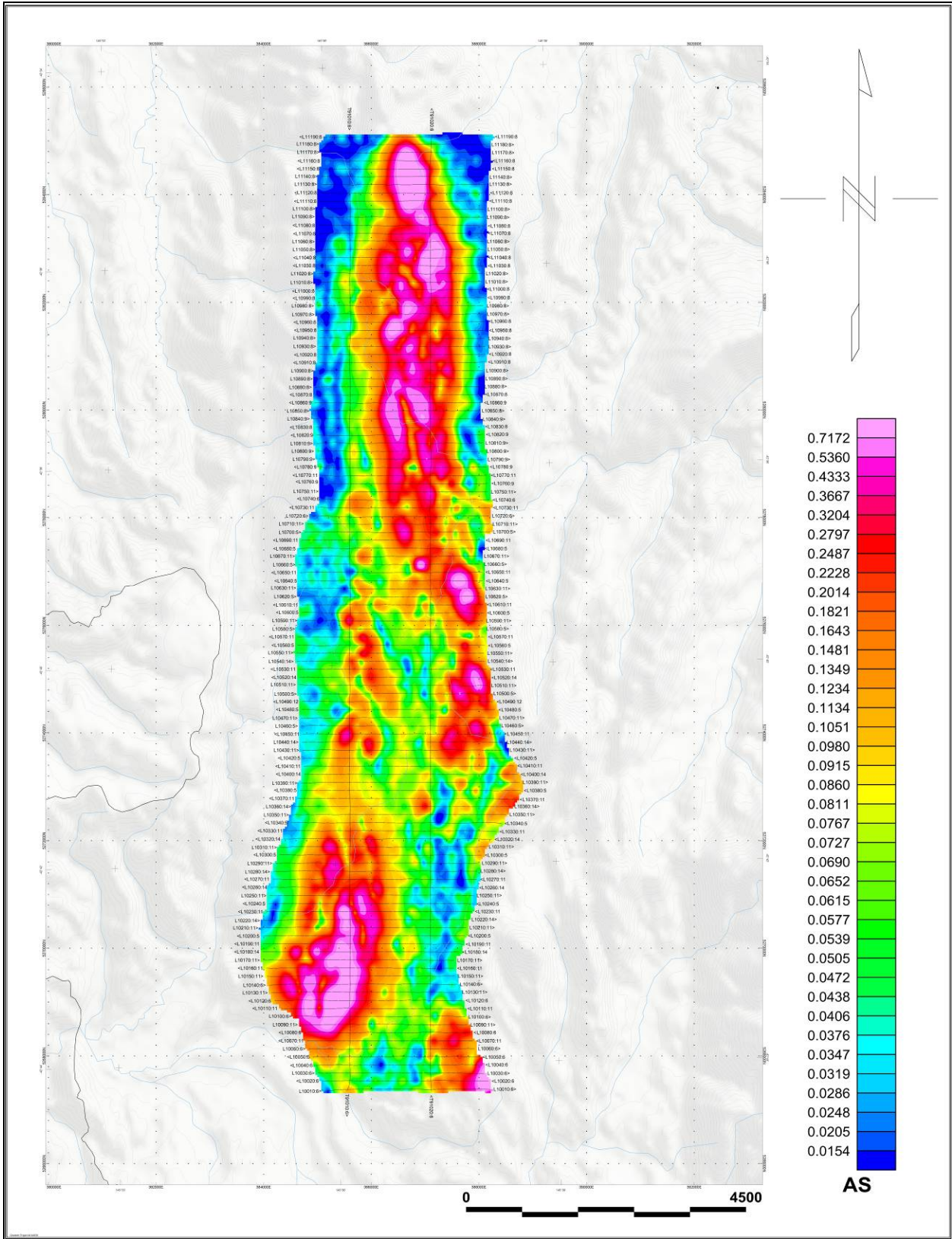
Daguilar Block – Analytic Signal (AS)
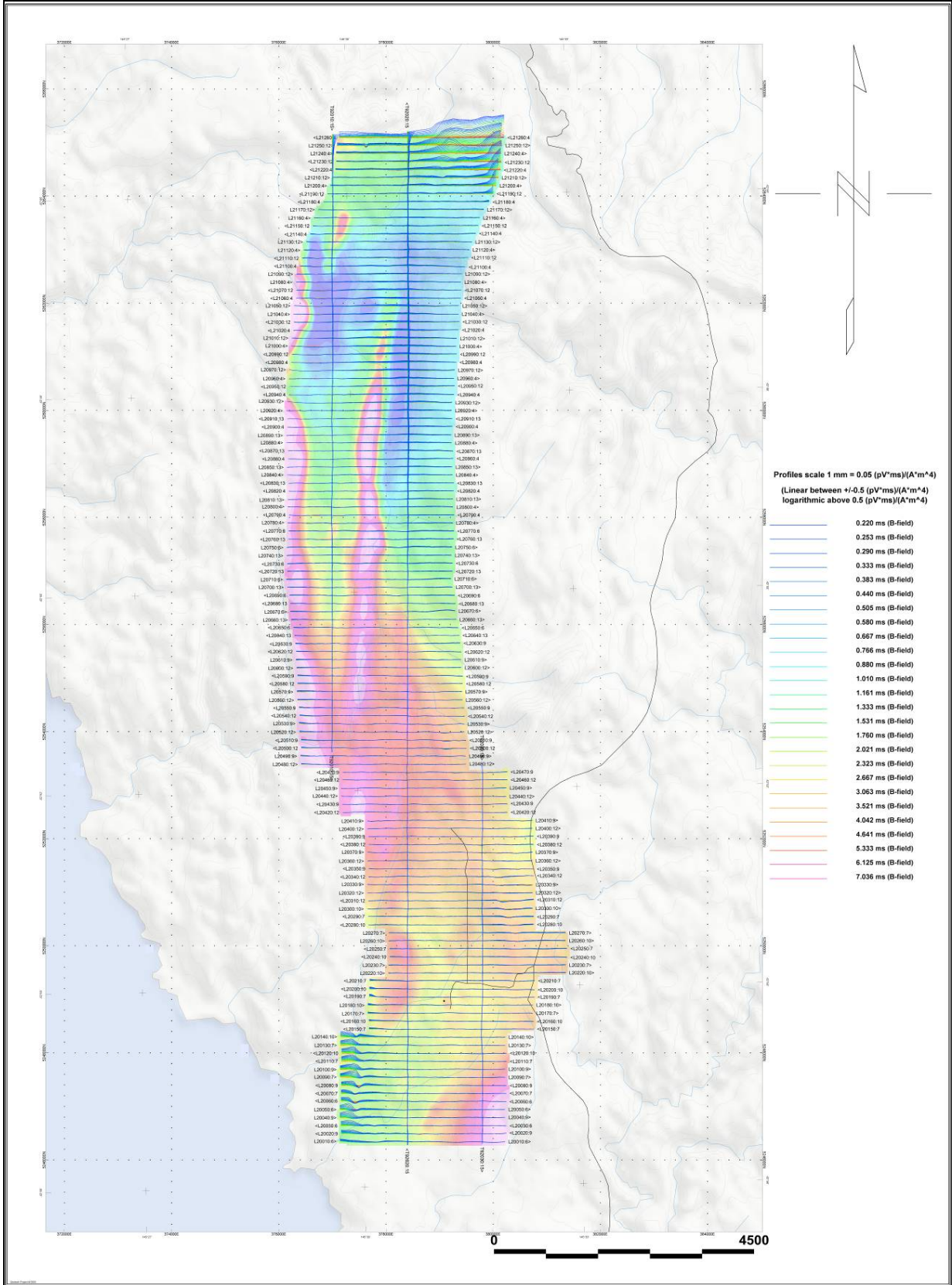
WartHill Block - VTEM B-Field Z Component Profiles, Time Gates 0.220 to 7.036 ms
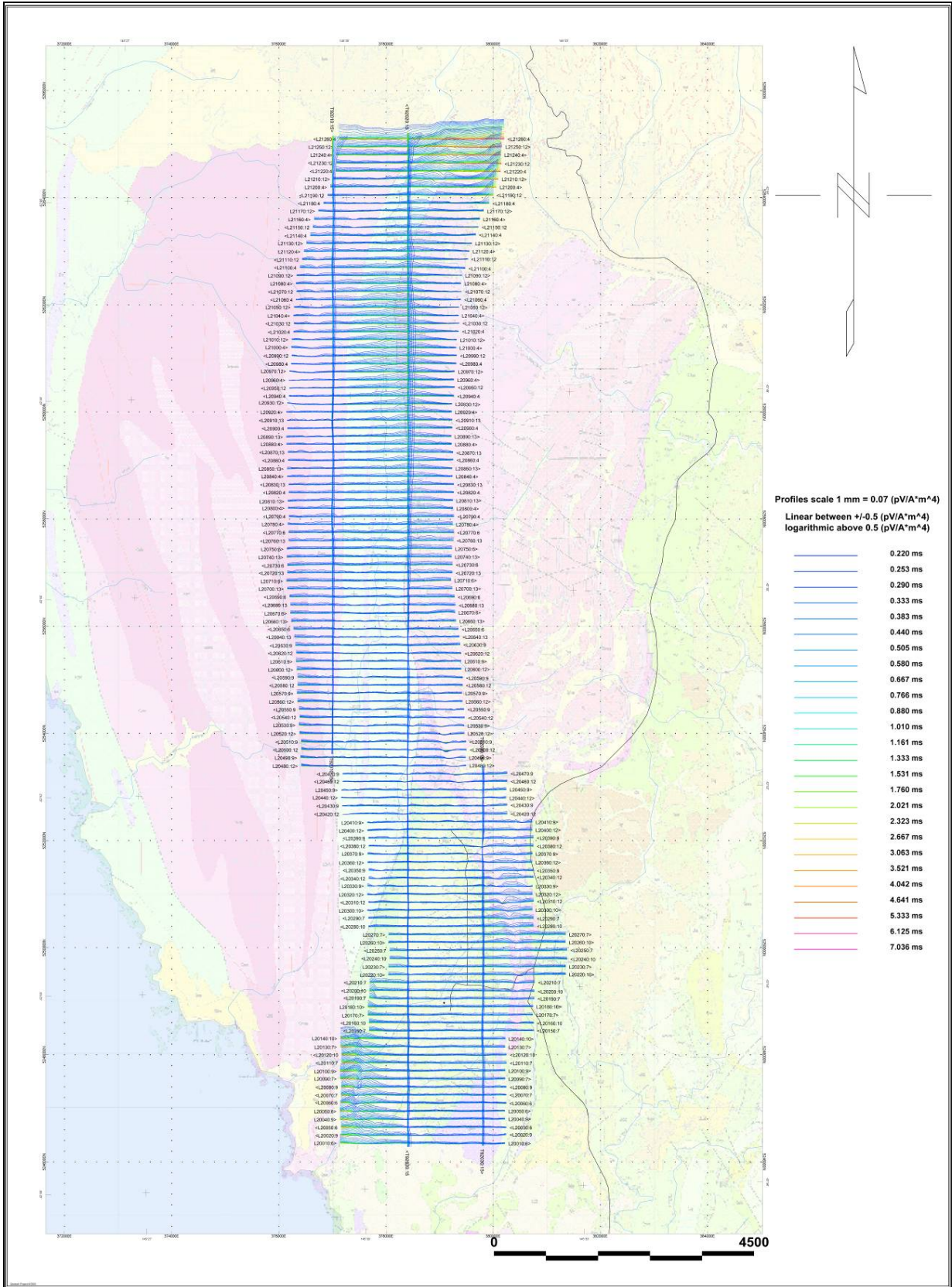
WartHill Block - VTEM dB/dt Z Component Profiles, Time Gates 0.220 to 7.036 ms

Profiles scale 1 mm = 0.07 (pV/A*m^4)

Linear between +/-0.5 (pV/A*m^4)
logarithmic above 0.5 (pV/A*m^4)

	0.220 ms
	0.253 ms
	0.290 ms
	0.333 ms
	0.383 ms
	0.440 ms
	0.505 ms
	0.580 ms
	0.667 ms
	0.766 ms
	0.880 ms
	1.010 ms
	1.161 ms
	1.333 ms
	1.531 ms
	1.760 ms
	2.021 ms
	2.323 ms
	2.667 ms
	3.063 ms
	3.521 ms
	4.042 ms
	4.641 ms
	5.333 ms
	6.125 ms
	7.036 ms

0   4500

Geotech Ltd.

WartHill Block - VTEM B-Field Z Component Channel 30, Time Gate 0.880 ms

Geotech Ltd.
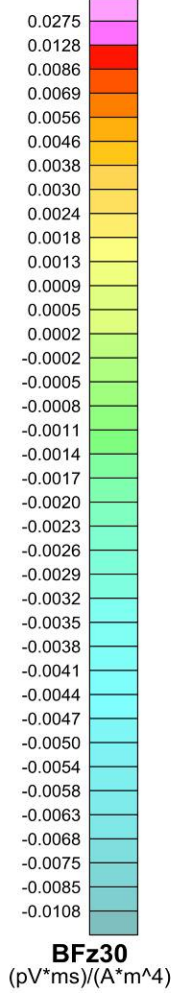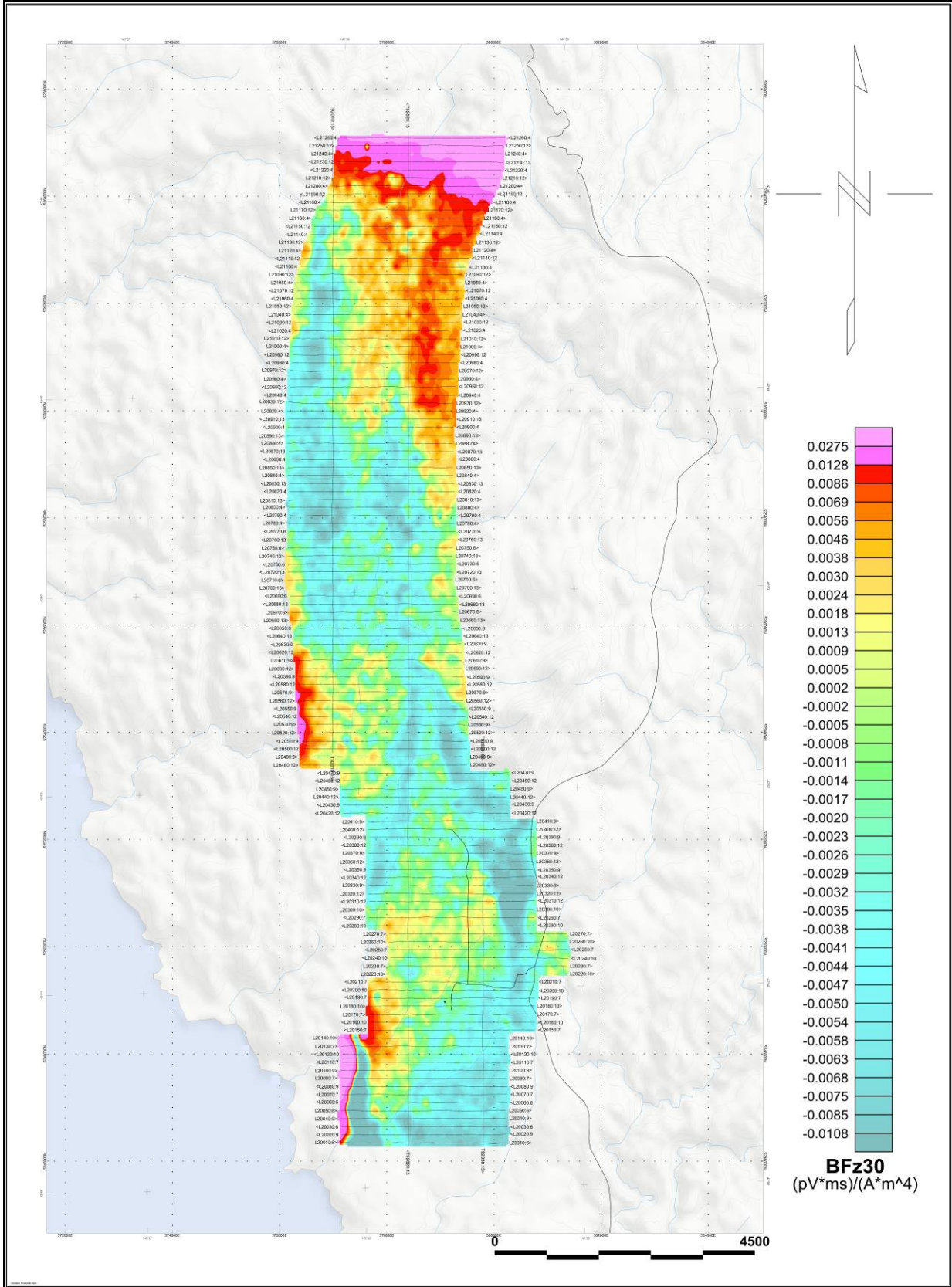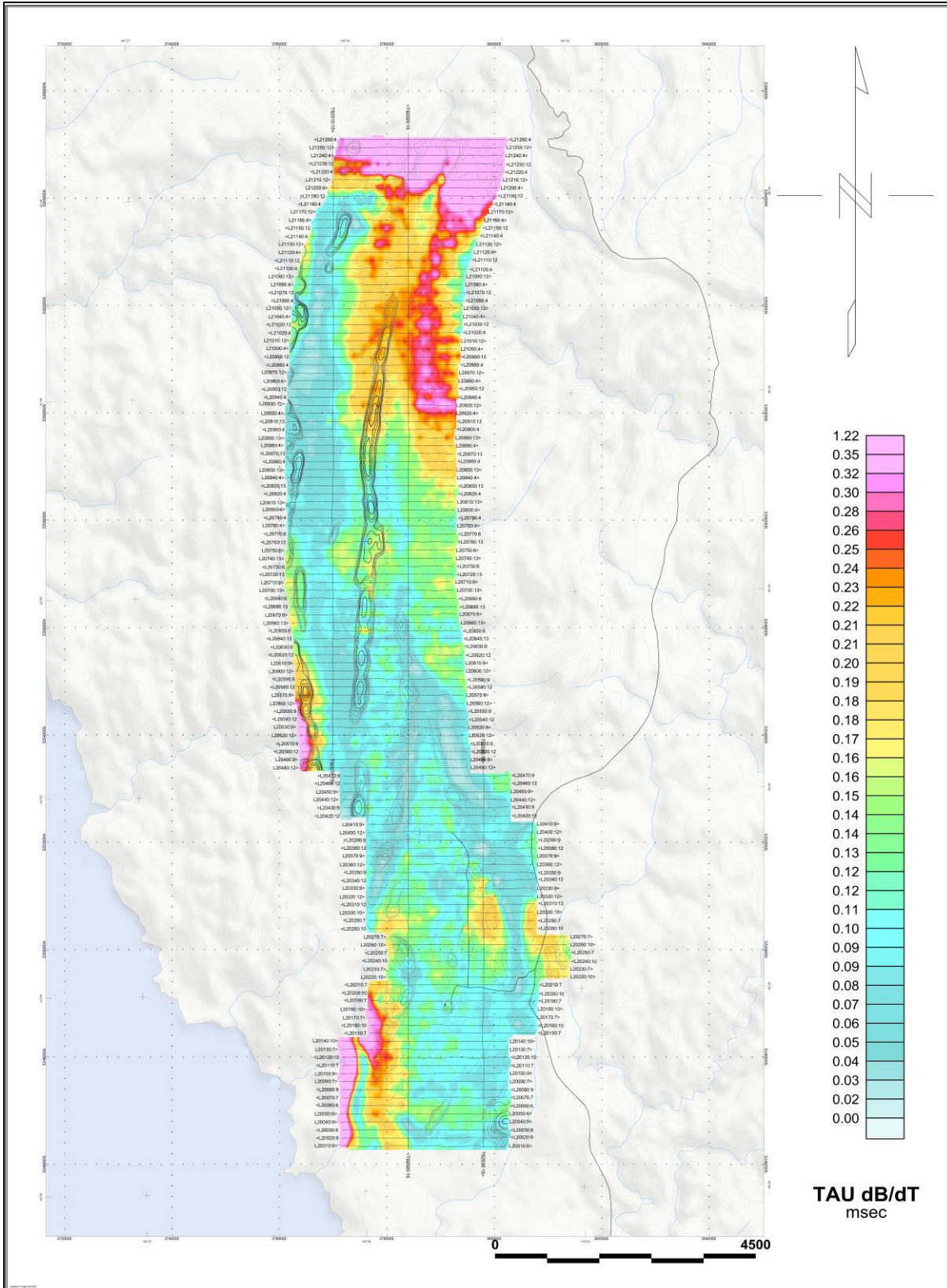
WartHill Block - dB/dt Calculated Time Constant (Tau) with contours of anomaly areas of the Calculated Vertical Derivative of TMI

TAU dB/dT
msec
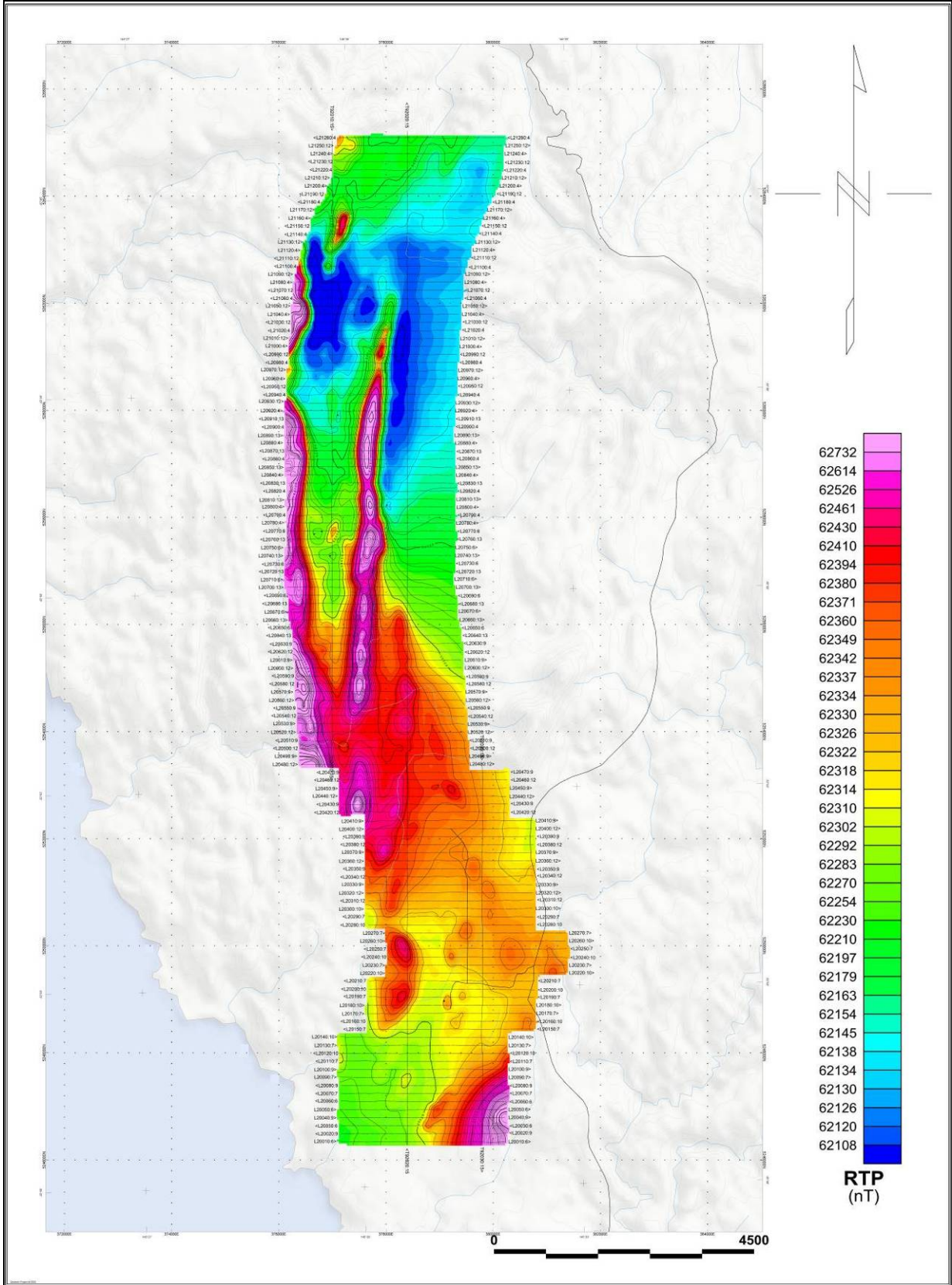
WartHill Block - Reduced to Pole of TMI (RTP)

WartHill Block – Analytic Signal (AS)

Profiles scale 1 mm = 0.04 (pV*ms)/(A*m^4)

(Linear between +/-0.5 (pV*ms)/(A*m^4)
logarithmic above 0.5 (pV*ms)/(A*m^4)

	0.220 ms (B-field)
	0.253 ms (B-field)
	0.290 ms (B-field)
	0.333 ms (B-field)
	0.383 ms (B-field)
	0.440 ms (B-field)
	0.505 ms (B-field)
	0.580 ms (B-field)
	0.667 ms (B-field)
	0.766 ms (B-field)
	0.880 ms (B-field)
	1.010 ms (B-field)
	1.161 ms (B-field)
	1.333 ms (B-field)
	1.531 ms (B-field)
	1.760 ms (B-field)
	2.021 ms (B-field)
	2.323 ms (B-field)
	2.667 ms (B-field)
	3.063 ms (B-field)
	3.521 ms (B-field)
	4.042 ms (B-field)
	4.641 ms (B-field)
	5.333 ms (B-field)
	6.125 ms (B-field)
	7.036 ms (B-field)

0   1500

Moores Block - VTEM B-Field Z Component Profiles, Time Gates 0.220 to 7.036 ms

Moores Block - VTEM dB/dt Z Component Profiles, Time Gates 0.220 to 7.036 ms
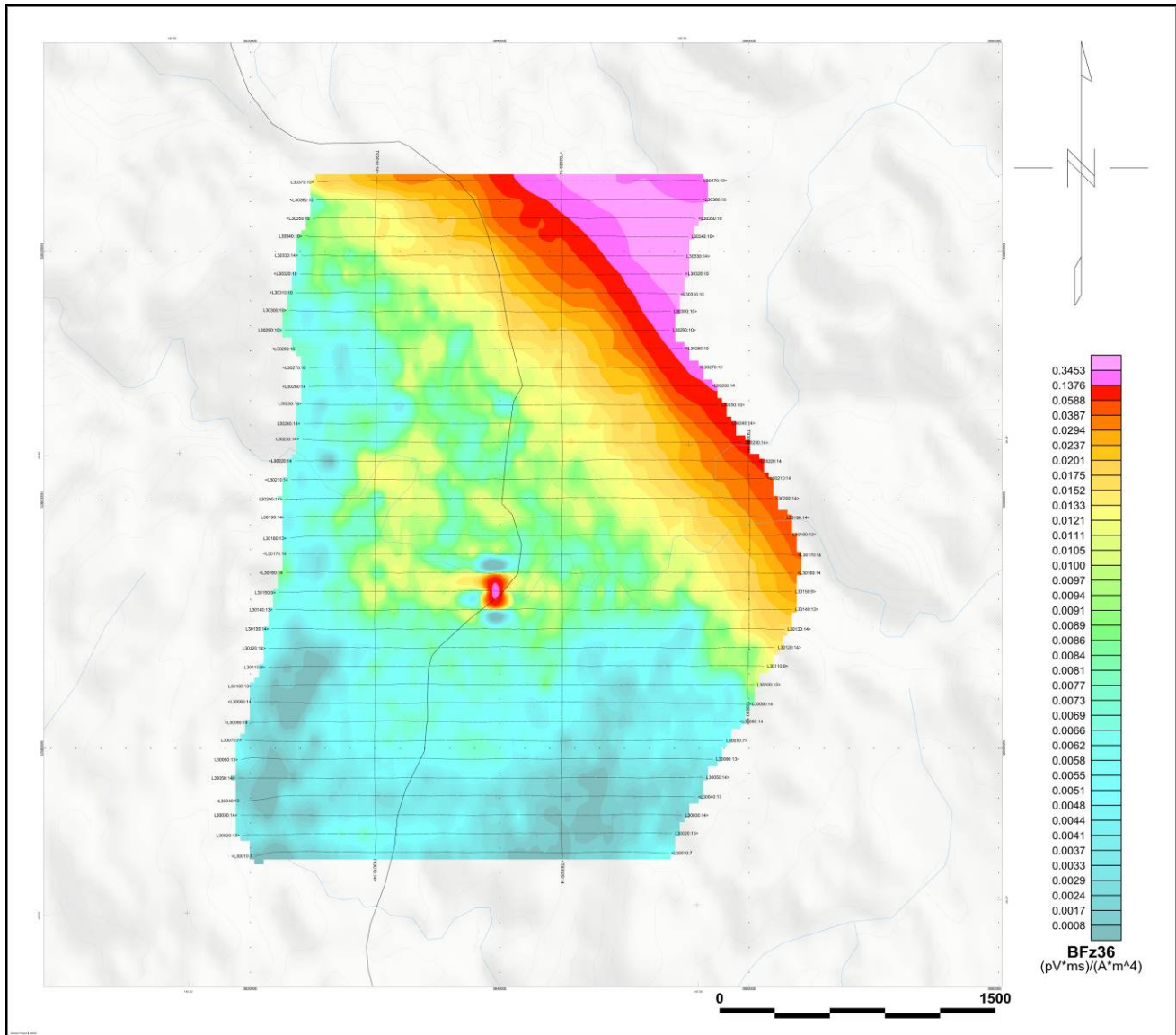
Moores Block - VTEM B-Field Z Component Channel 36, Time Gate 2.021 ms
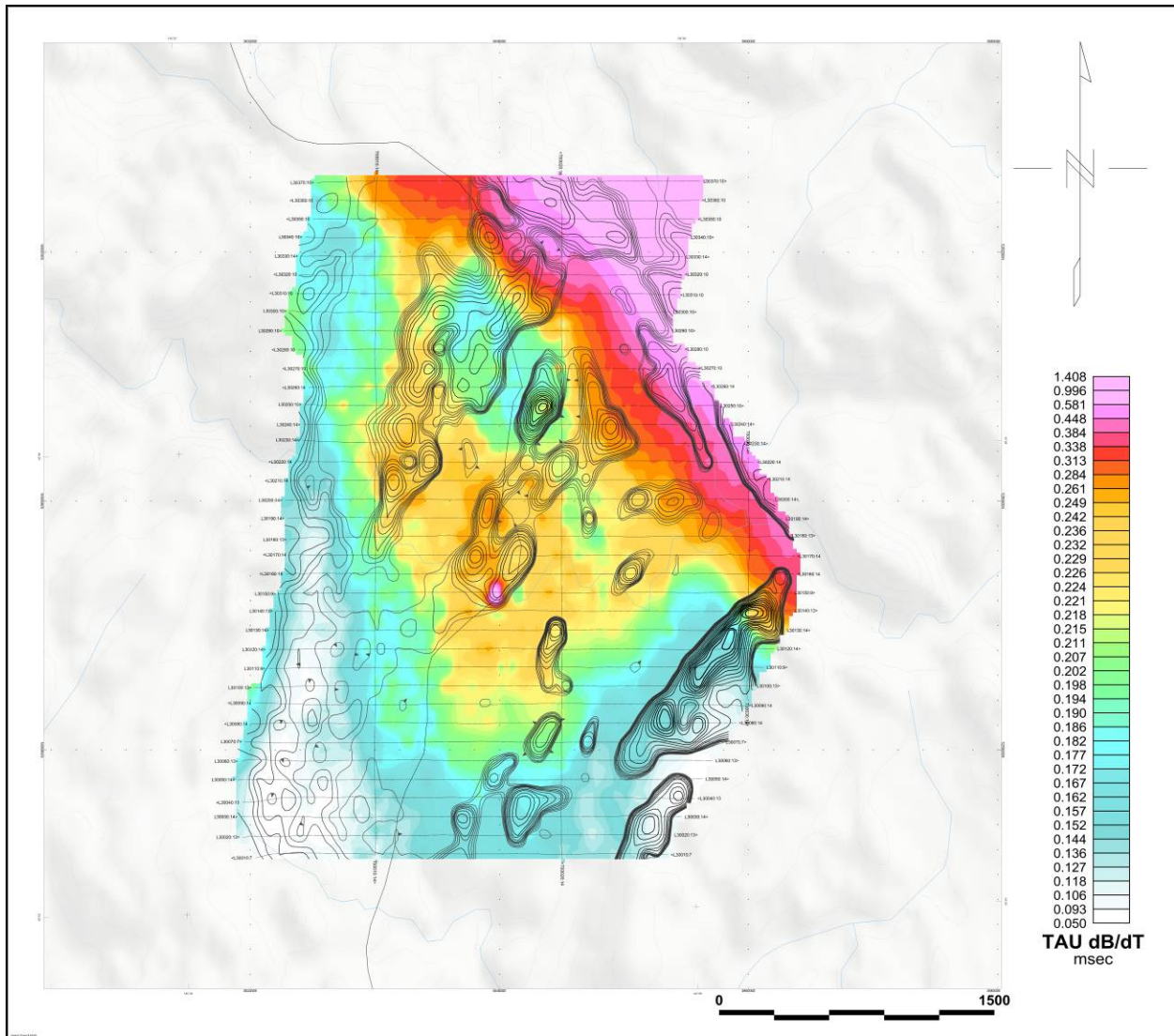
Moores Block - dB/dt Calculated Time Constant (Tau) with contours of anomaly areas of the Calculated Vertical Derivative of TMI
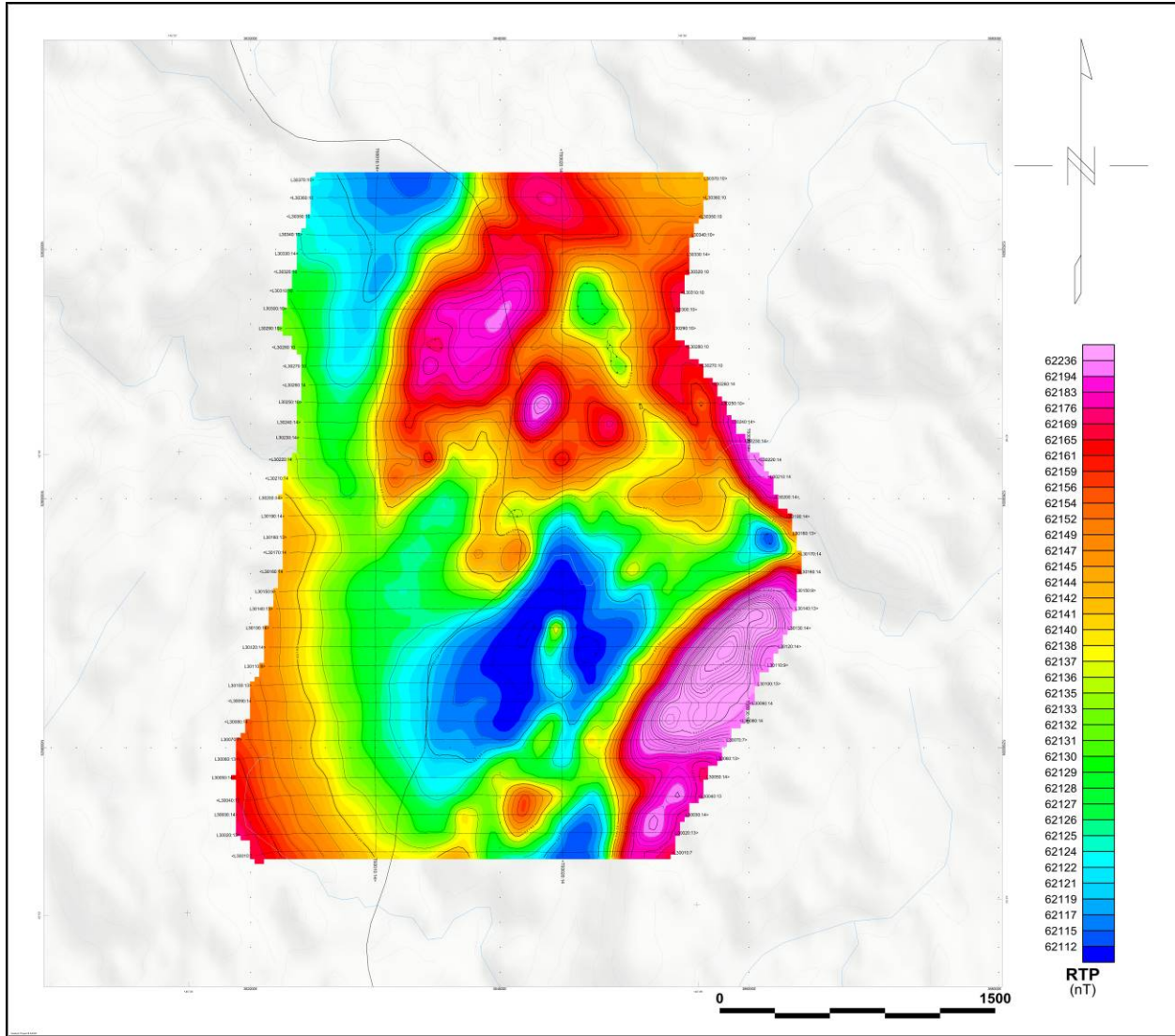
Moores Block - Reduced to Pole of TMI (RTP)
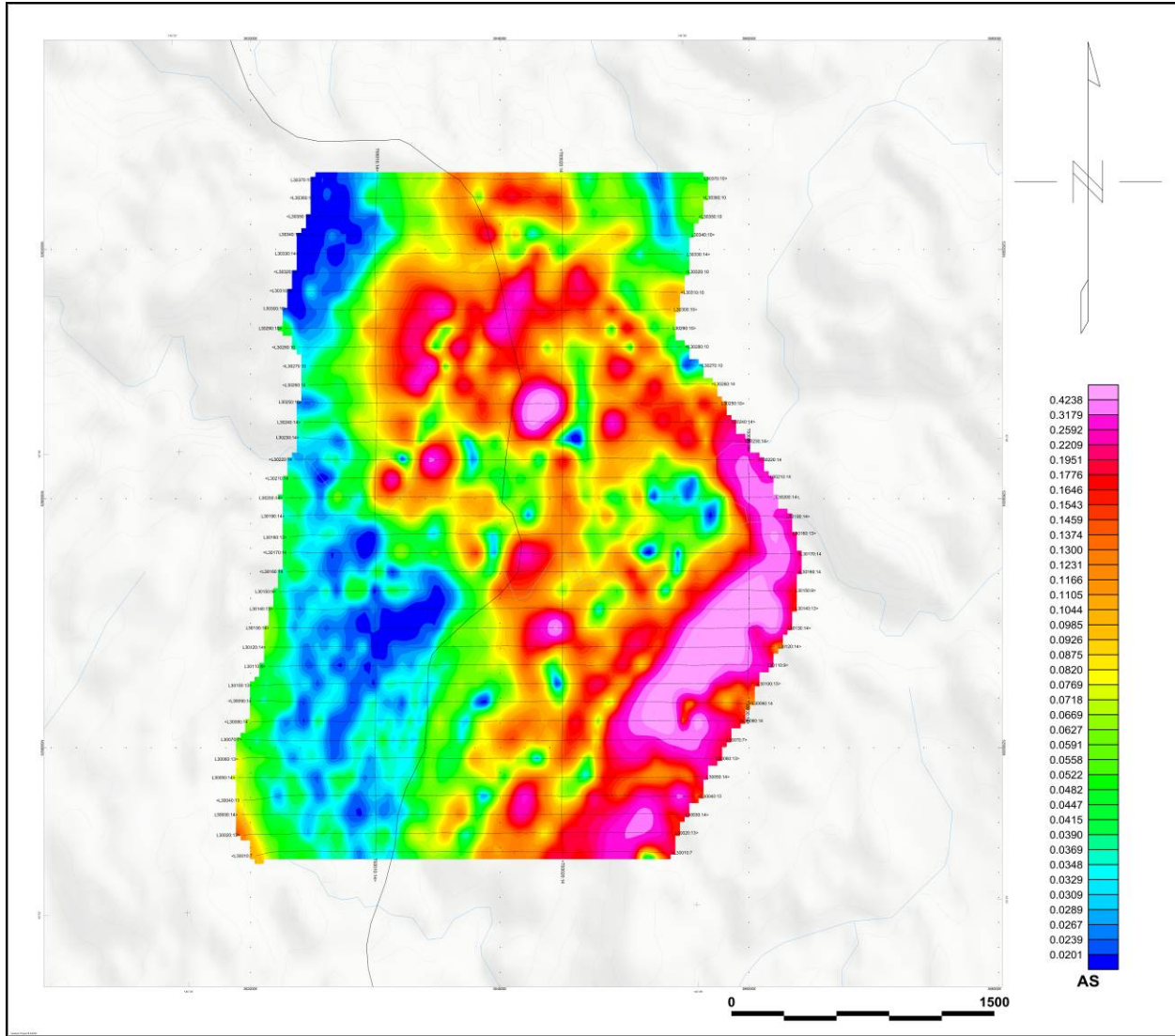
Moores Block - Analytic Signal (AS)

RESISTIVITY DEPTH IMAGE (RDI) MAPS

3D Resistivity Depth Images (RDI) (Daguilar)

AA926_Frontier_Daguilar_RDI_Apparent_Resistivity
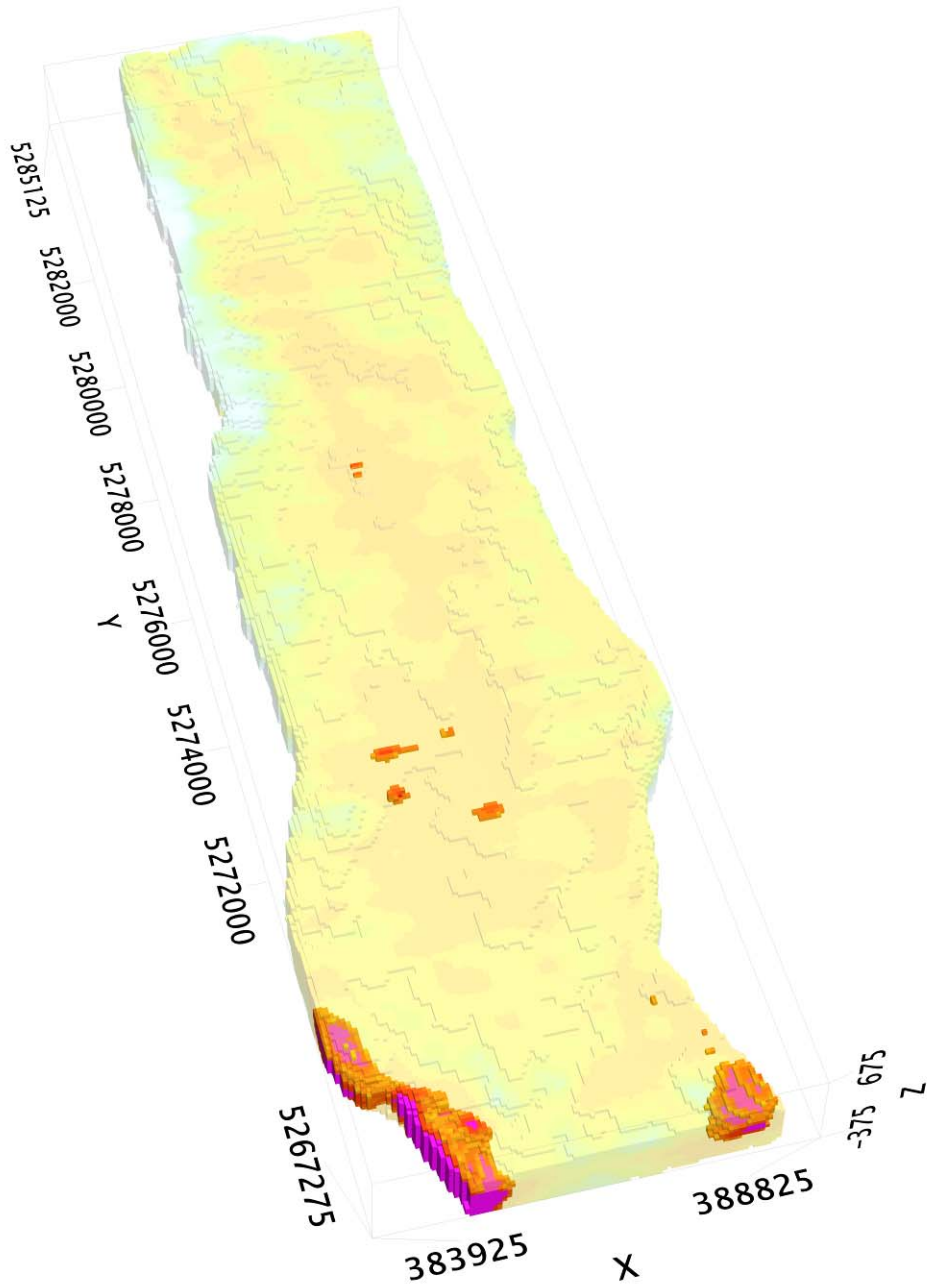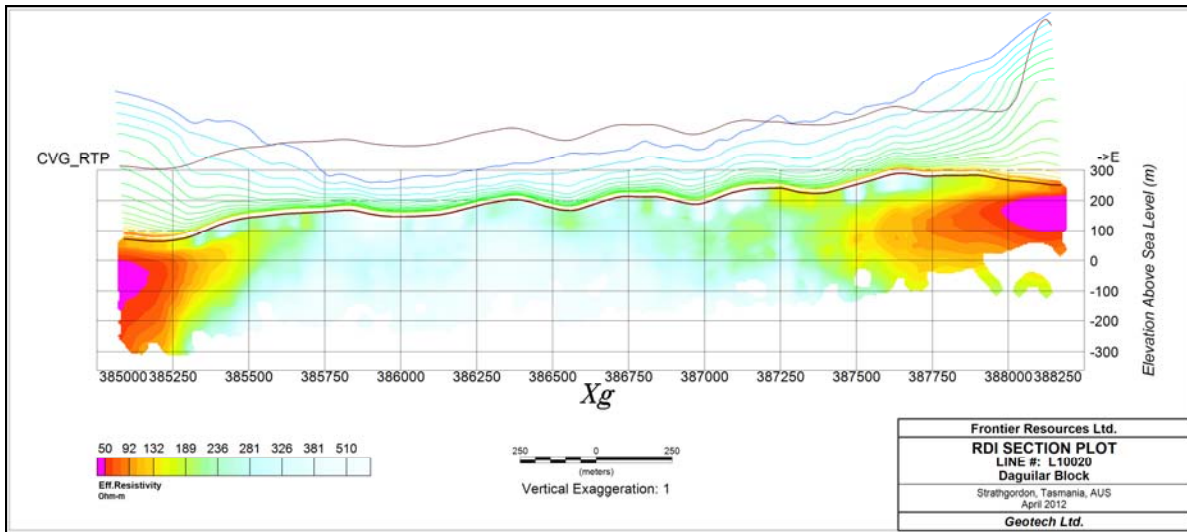
L10020
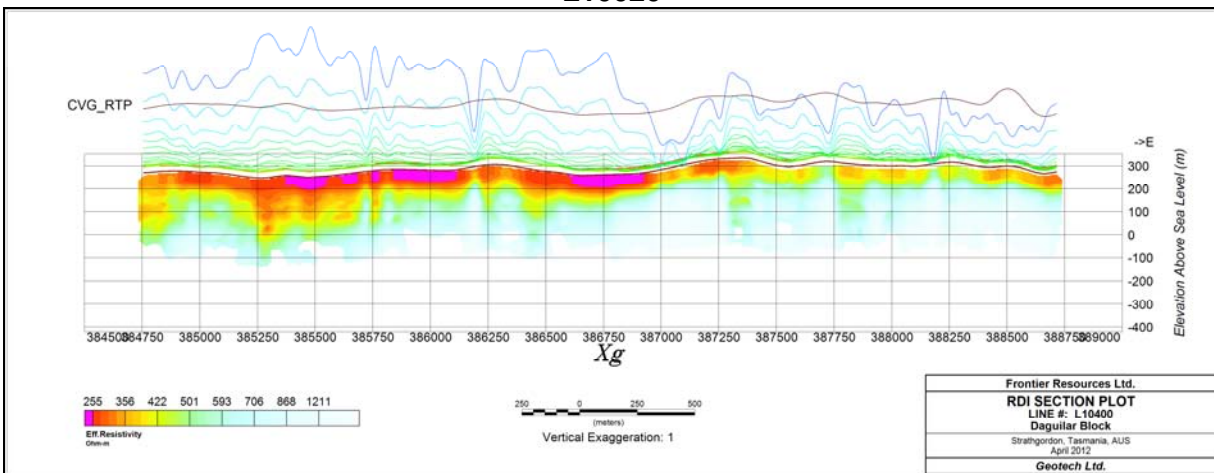
L10400
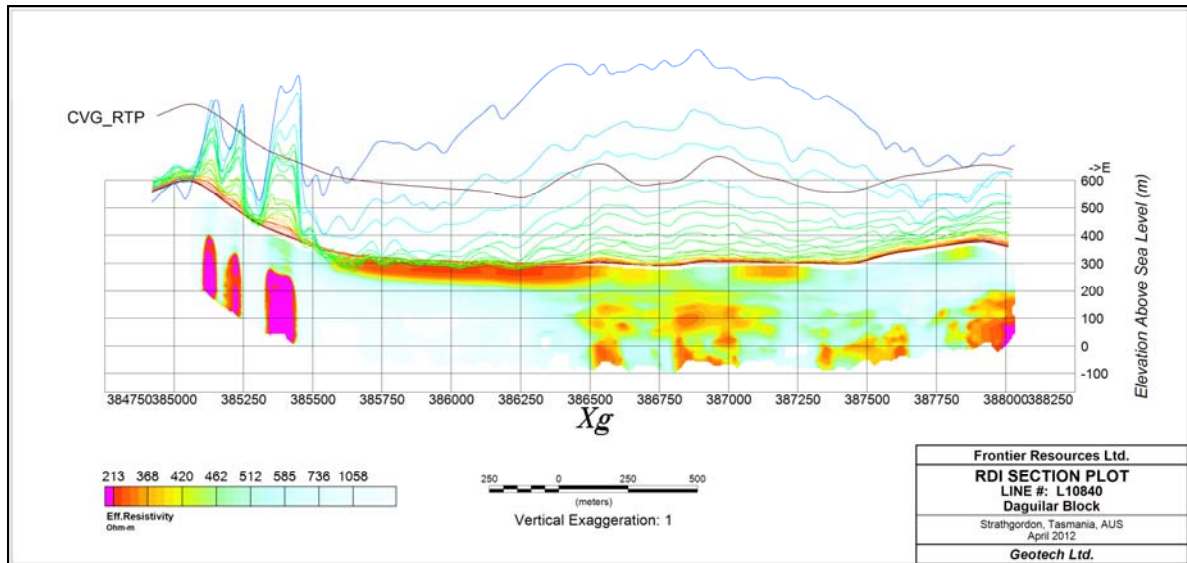
L10840

3D Resistivity Depth Images (RDI) (WartHill)

AA926_Frontier_WartHill_RDI_Apparent_Resistivity
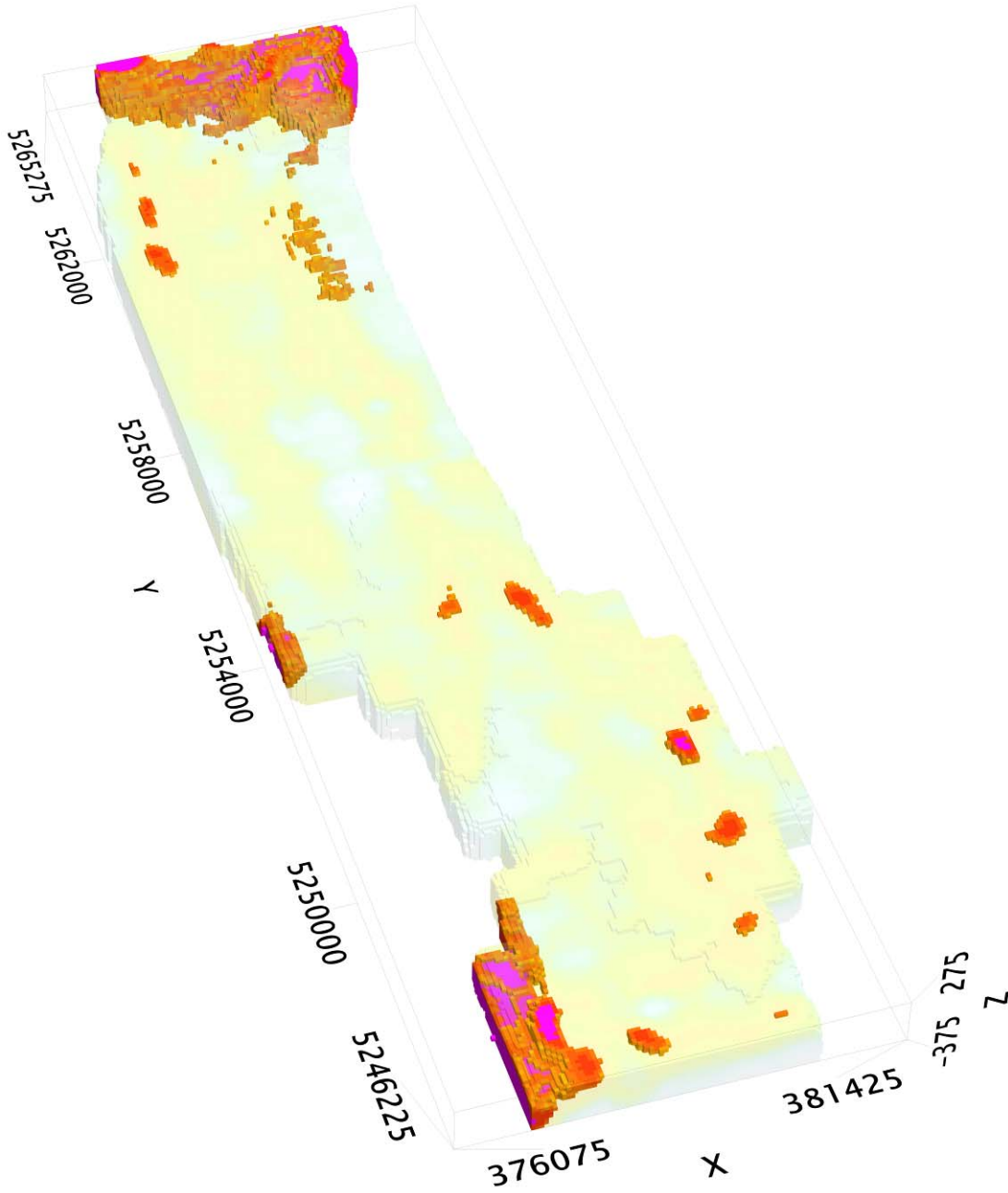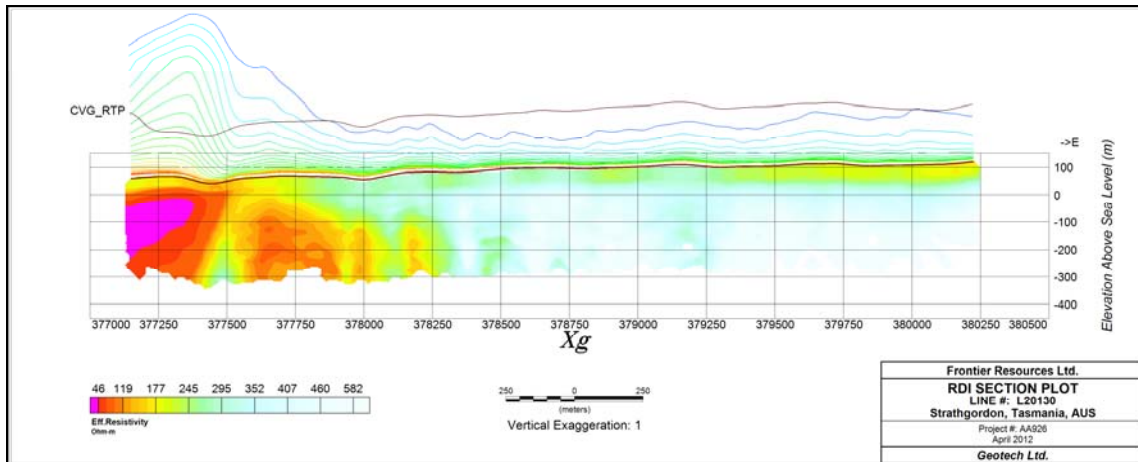
RDI Sections - Line 20130 (WartHill)
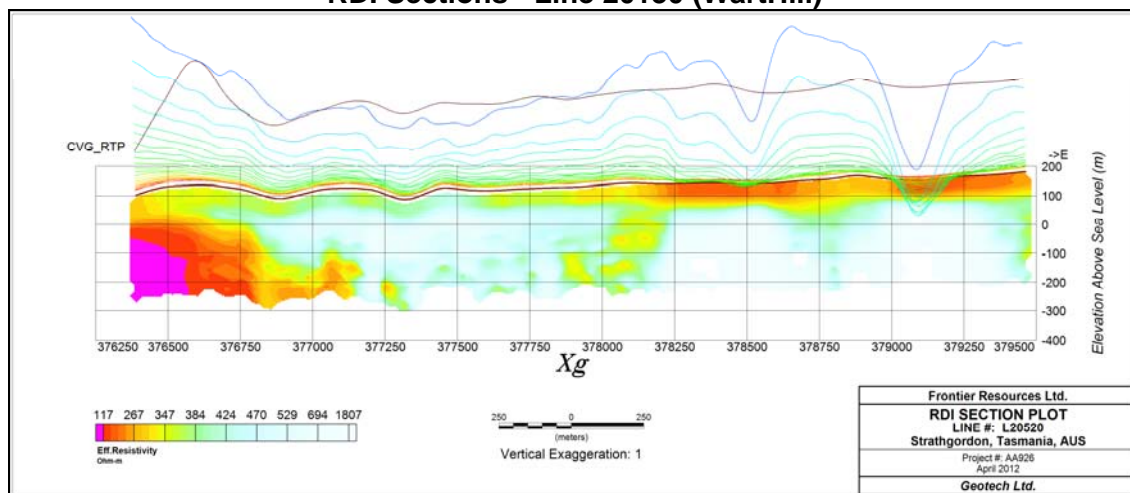
RDI Sections - Line 20520 (WartHill)
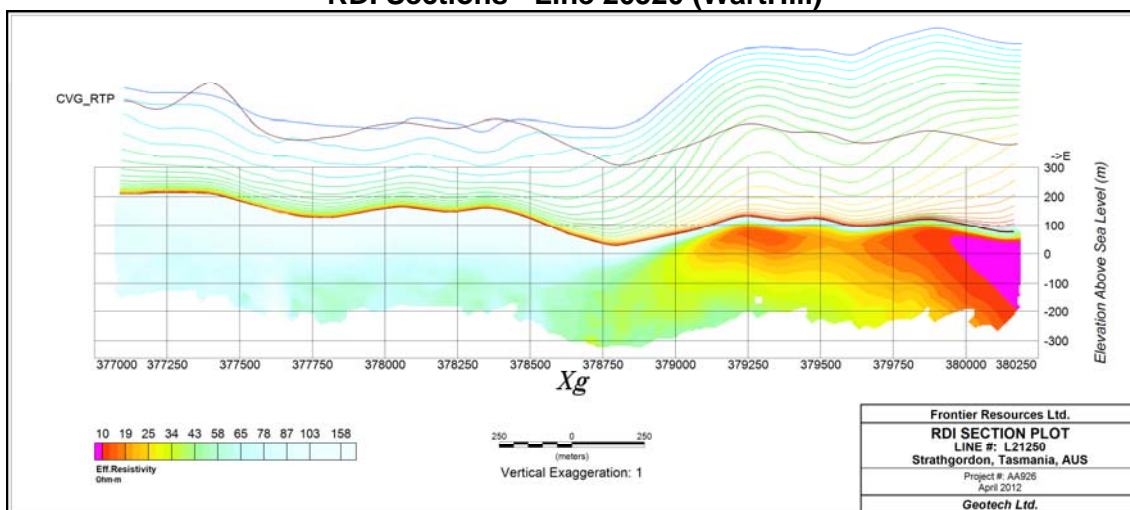
RDI Sections - Line 21250 (WartHill)

3D Resistivity Depth Images (RDI) (Moores)

AA926_Frontier_Moores_RDI_Apparent_Resistivity
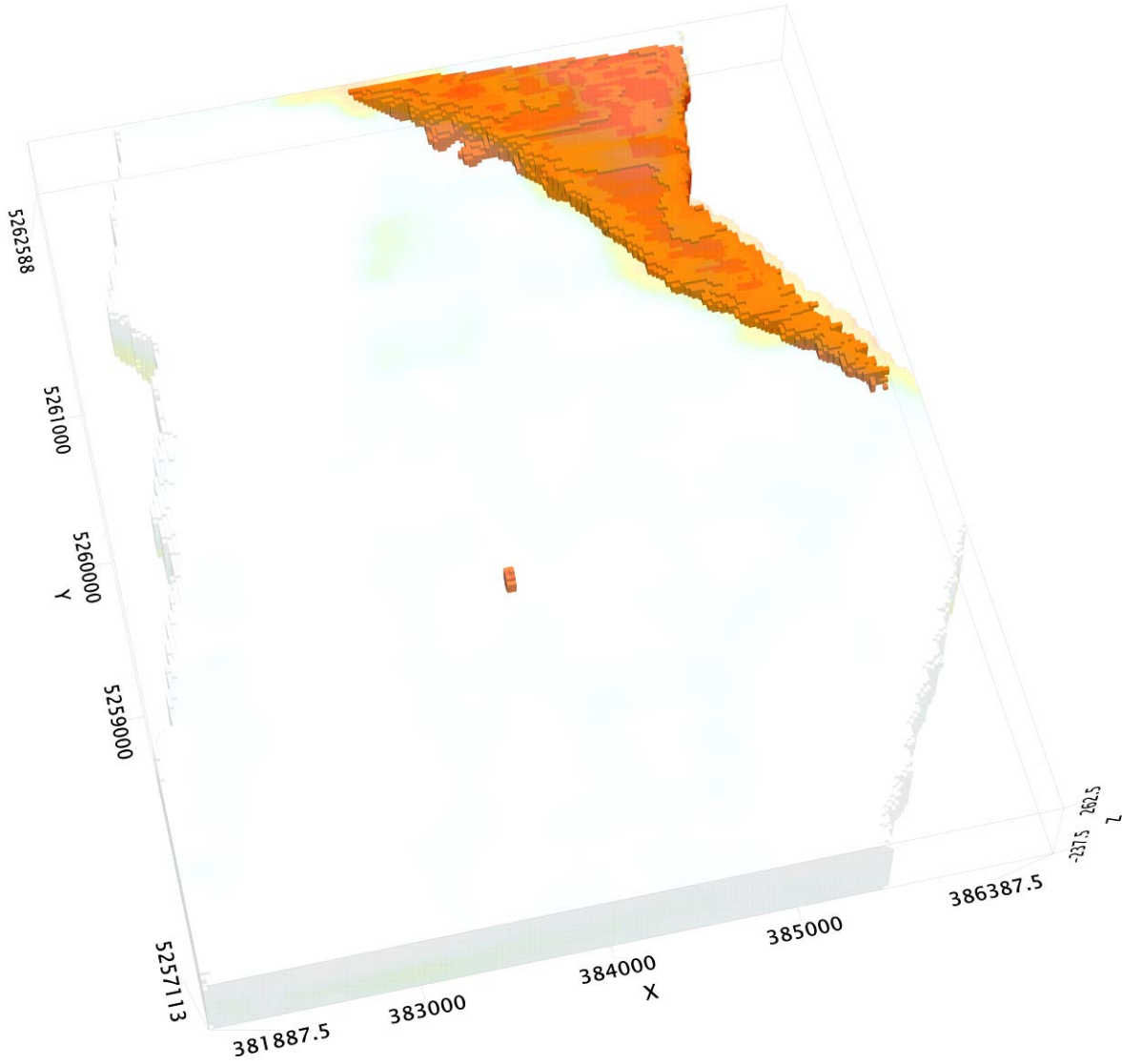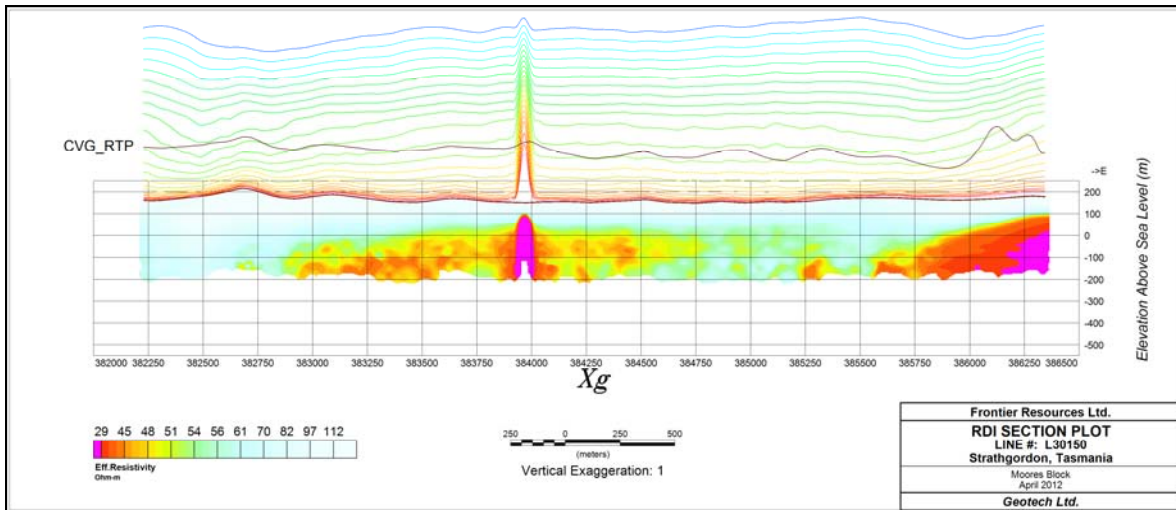
RDI Sections - Line 30150 (Moores)
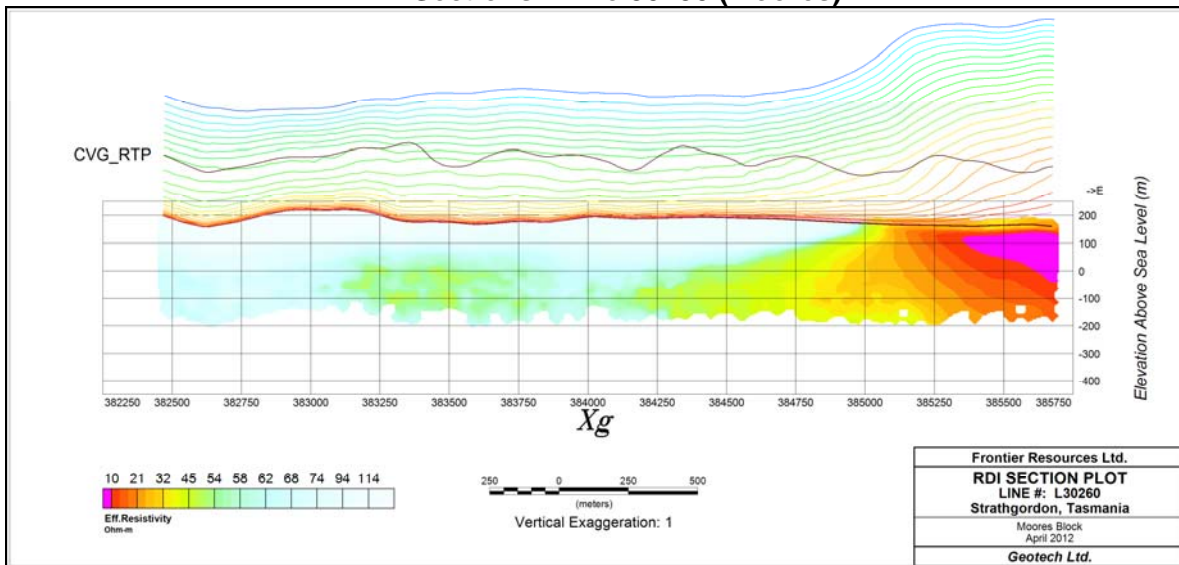
RDI Sections - Line 30260 (Moores)
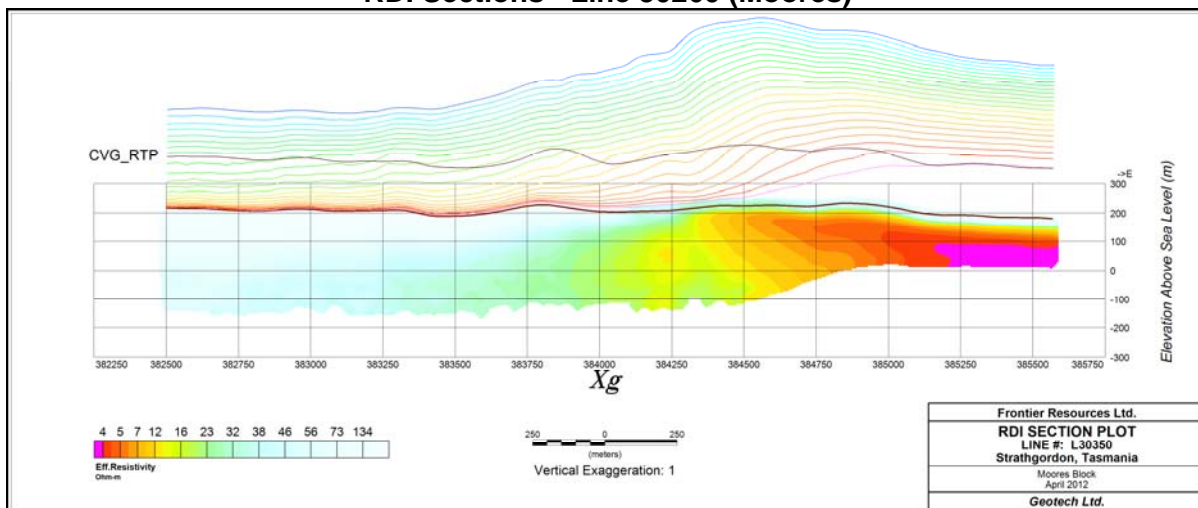
RDI Sections - Line 30350 (Moores)

APPENDIX D

GENERALIZED MODELING RESULTS OF THE VTEM SYSTEM

Introduction

The VTEM system is based on a concentric or central loop design, whereby, the receiver is positioned at the centre of a transmitter loop that produces a primary field. The wave form is a bi-polar, modified square wave with a turn-on and turn-off at each end.

During turn-on and turn-off, a time varying field is produced (dB/dt) and an electro-motive force (emf) is created as a finite impulse response. A current ring around the transmitter loop moves outward and downward as time progresses. When conductive rocks and mineralization are encountered, a secondary field is created by mutual induction and measured by the receiver at the centre of the transmitter loop.

Efficient modeling of the results can be carried out on regularly shaped geometries, thus yielding close approximations to the parameters of the measured targets. The following is a description of a series of common models made for the purpose of promoting a general understanding of the measured results.

A set of models has been produced for the Geotech VTEM® system dB/dT Z and X components (see models D1 to D15). The Maxwell [TM] modeling program (EMIT Technology Pty. Ltd. Midland, WA, AU) used to generate the following responses assumes a resistive half-space. The reader is encouraged to review these models, so as to get a general understanding of the responses as they apply to survey results. While these models do not begin to cover all possibilities, they give a general perspective on the simple and most commonly encountered anomalies.

As the plate dips and departs from the vertical position, the peaks become asymmetrical.

As the dip increases, the aspect ratio (Min/Max) decreases and this aspect ratio can be used as an empirical guide to dip angles from near 90º to about 30º. The method is not sensitive enough where dips are less than about 30º.

Figure D-1: vertical thin plate

Figure D-2: inclined thin plate

Figure D-3: inclined thin plate

Figure D-4: horizontal thin plate

Figure D-5: horizontal thick plate (linear scale of the response)

**Figure D-6:** horizontal thick plate (log scale of the response)
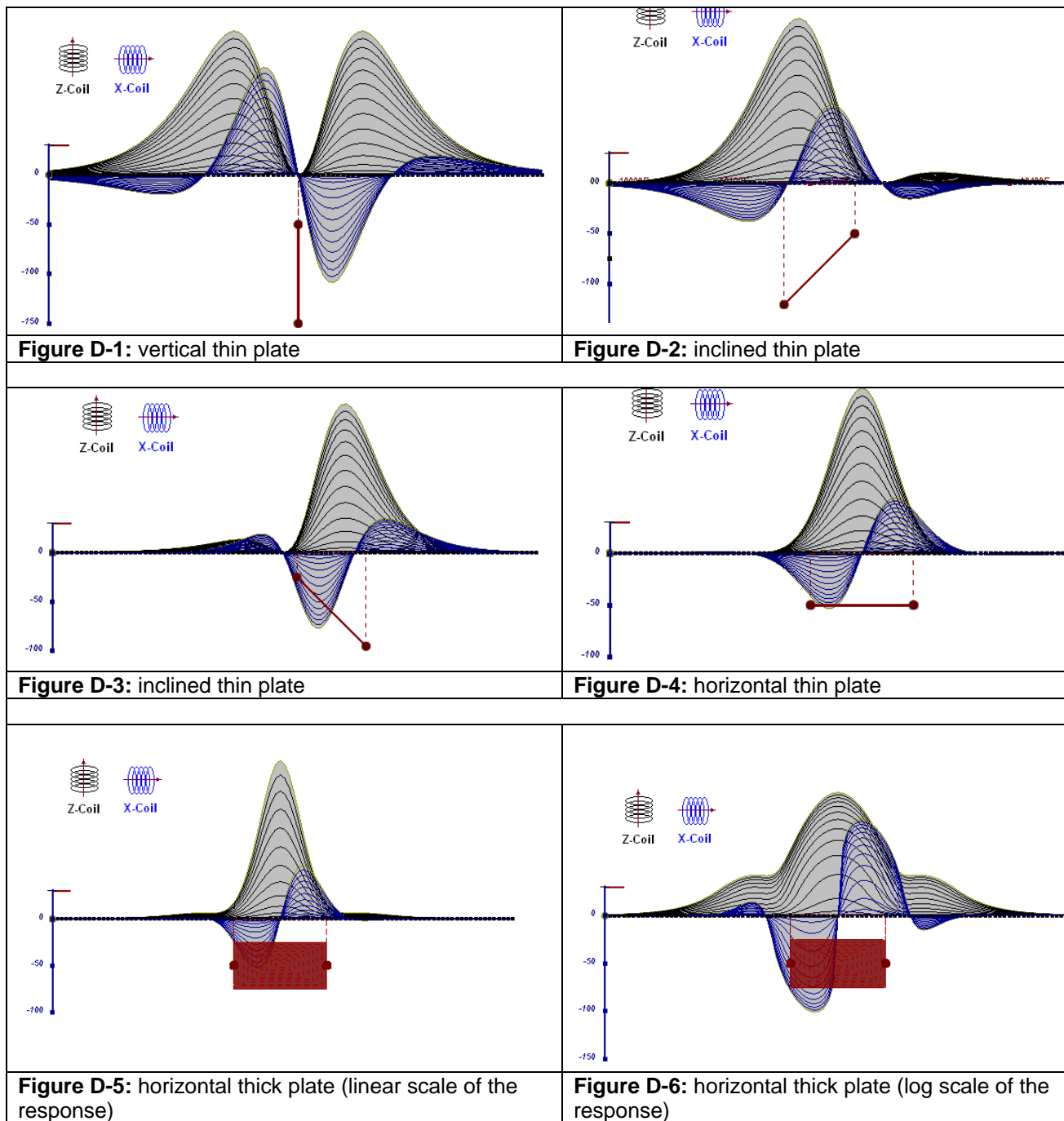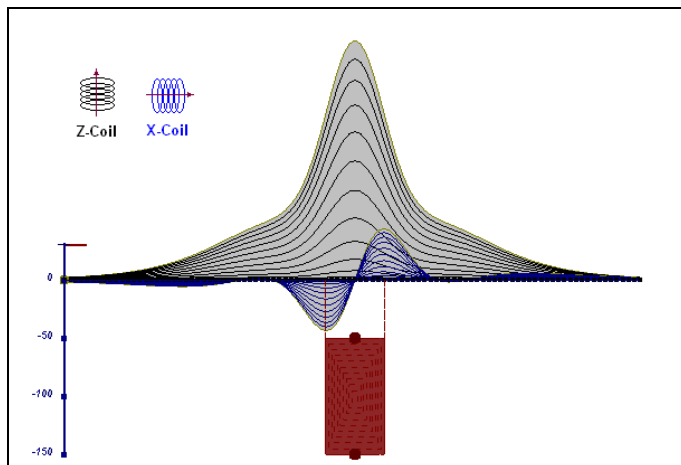
Figure D-7: vertical thick plate (linear scale of the response). 50 m depth
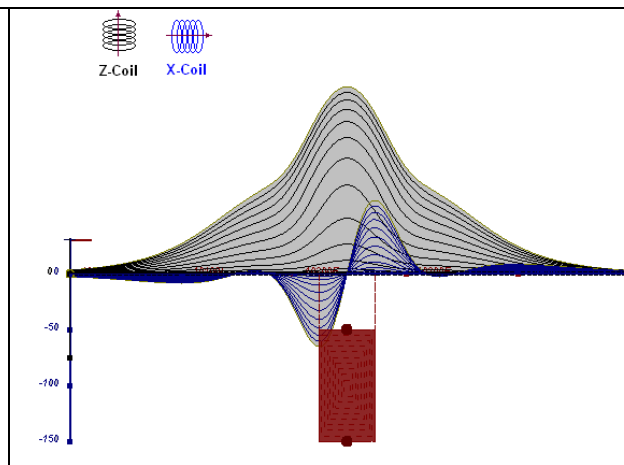
Figure D-8: vertical thick plate (log scale of the response). 50 m depth
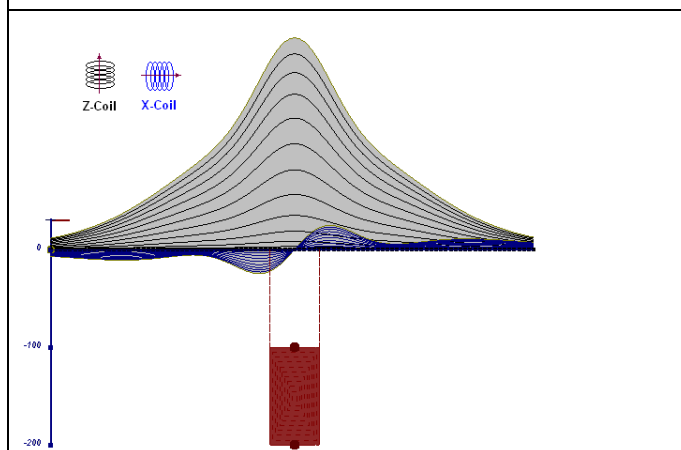
Figure D-9: vertical thick plate (linear scale of the response). 100 m depth
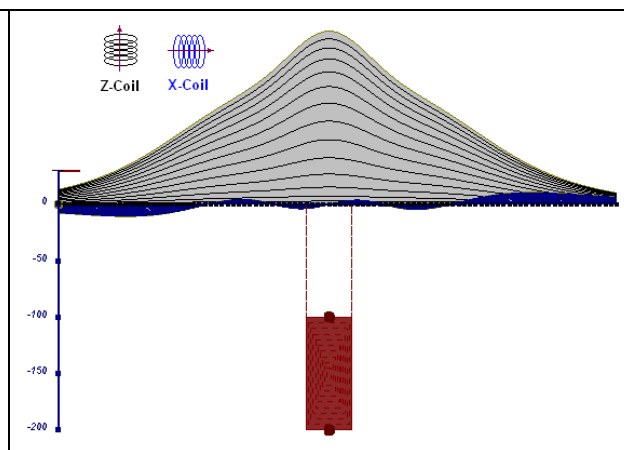
Figure D-10: vertical thick plate (linear scale of the response). Depth/hor.thickness=2.5
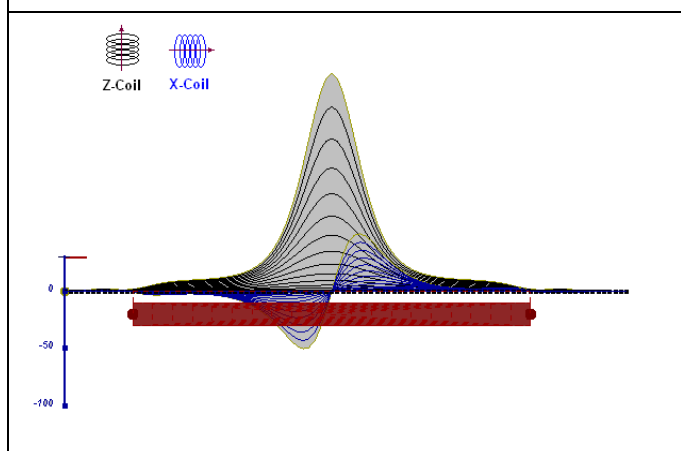
Figure D-10: horizontal thick plate (linear scale of the response)
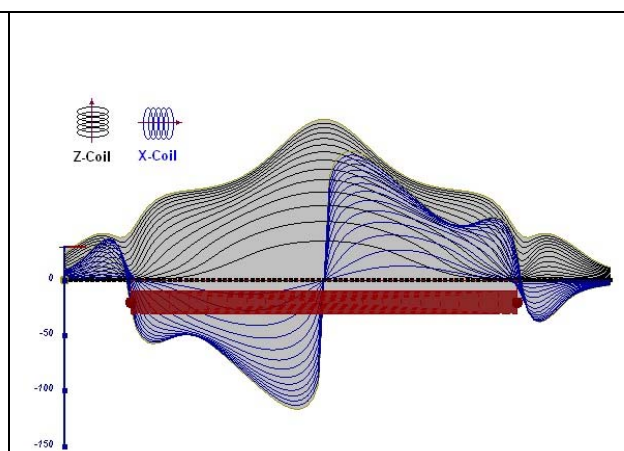
Figure D-11: horizontal thick plate (log scale of the response)
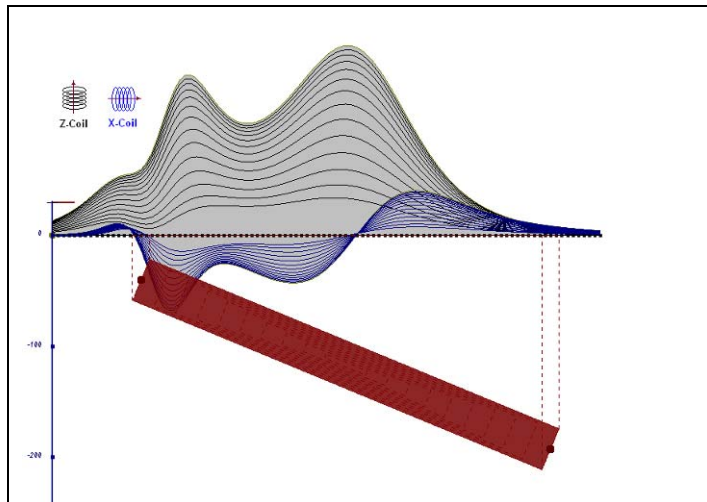
Figure D-12: inclined long thick plate
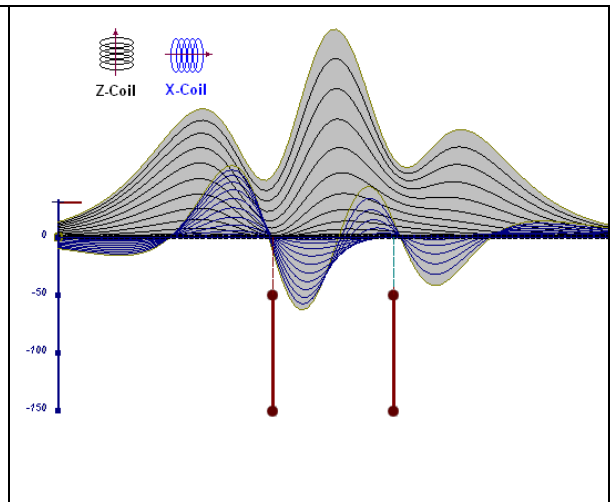
Figure D-13: two vertical thin plates
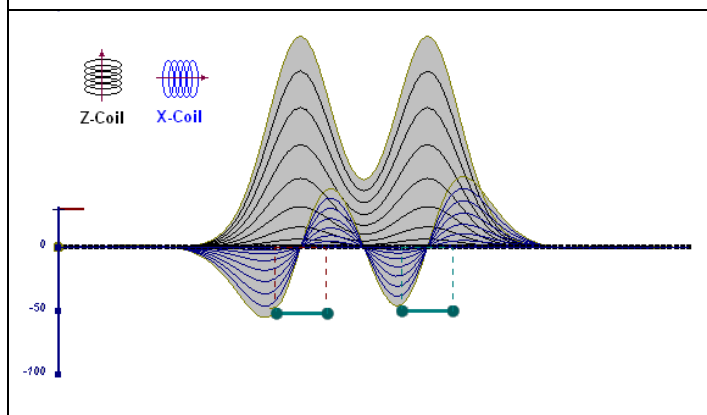
Figure D-14: two horizontal thin plates
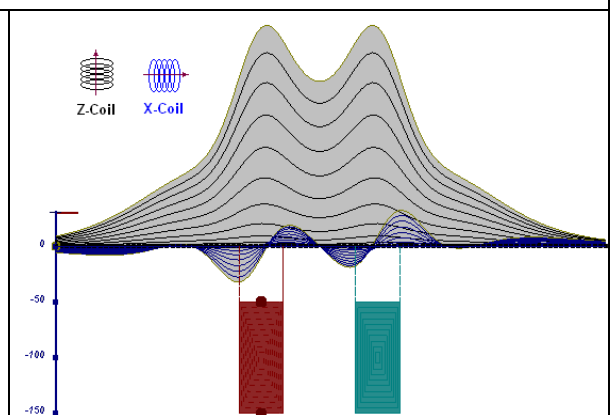
Figure D-15: two vertical thick plates

The same type of target but with different thickness, for example, creates different form of the response:

"thin"	10 m thickness	15 m thickness
18 m thickness	20 m thickness	30 m thickness
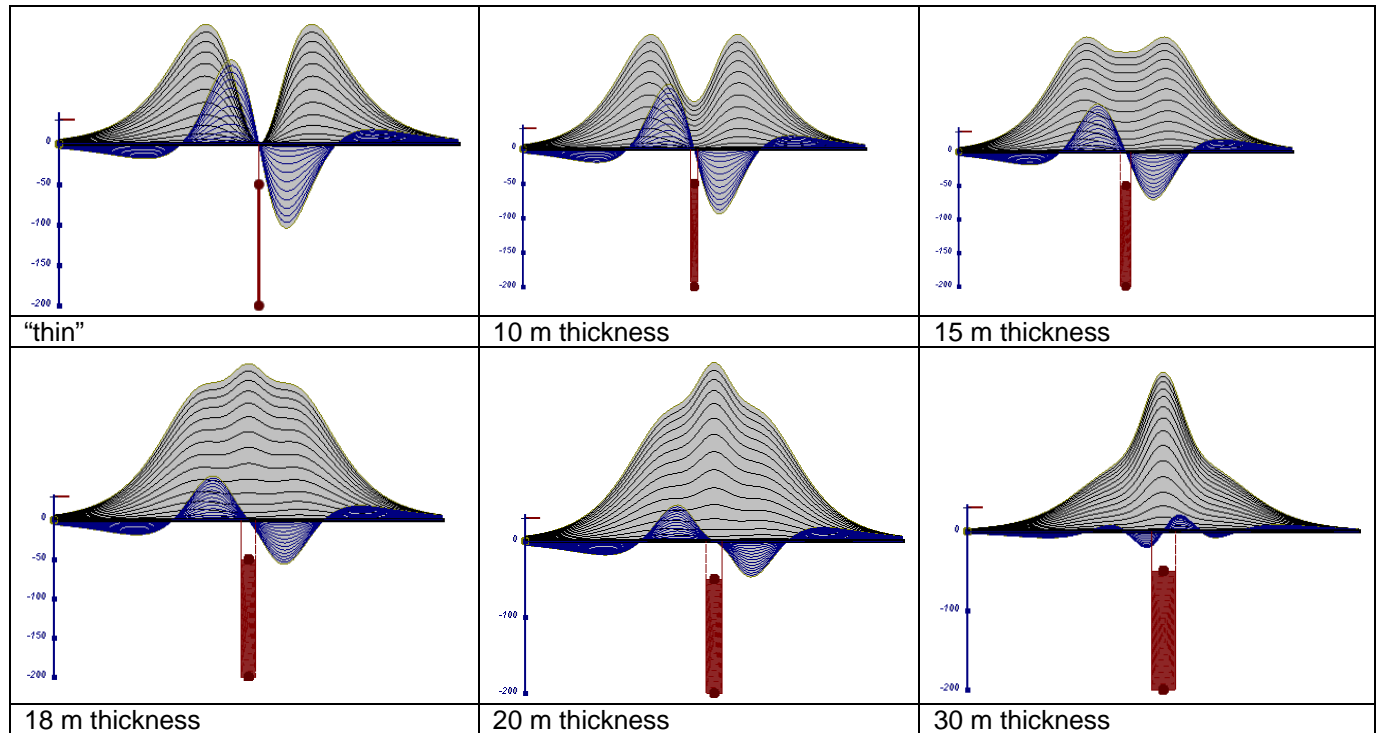
Figure D-16: Conductive vertical plate, depth 50 m, strike length 200 m, depth extend 150 m.

Alexander Prikhodko, PhD, P.Geo
Geotech Ltd.

September 2010

APPENDIX E

EM TIME CONSTANT (TAU) ANALYSIS

Estimation of time constant parameter[1] in transient electromagnetic method is one of the steps toward the extraction of the information about conductances beneath the surface from TEM measurements.

The most reliable method to discriminate or rank conductors from overburden, background or one and other is by calculating the EM field decay time constant (TAU parameter), which directly depends on conductance despite their depth and accordingly amplitude of the response.

Theory

As established in electromagnetic theory, the magnitude of the electro-motive force (emf) induced is proportional to the time rate of change of primary magnetic field at the conductor. This emf causes eddy currents to flow in the conductor with a characteristic transient decay, whose Time Constant (Tau) is a function of the conductance of the survey target or conductivity and geometry (including dimensions) of the target. The decaying currents generate a proportional secondary magnetic field, the time rate of change of which is measured by the receiver coil as induced voltage during the Off time.

The receiver coil output voltage (e_0) is proportional to the time rate of change of the secondary magnetic field and has the form,

$$e_0 \; \alpha \; (1 \, / \, \tau) \; e^{-(t/\tau)}$$

Where,
$\tau = L/R$ is the characteristic time constant of the target (TAU)
R = resistance
L = inductance

From the expression, conductive targets that have small value of resistance and hence large value of τ yield signals with small initial amplitude that decays relatively slowly with progress of time. Conversely, signals from poorly conducting targets that have large resistance value and small τ, have high initial amplitude but decay rapidly with time[1] (Figure E-1).
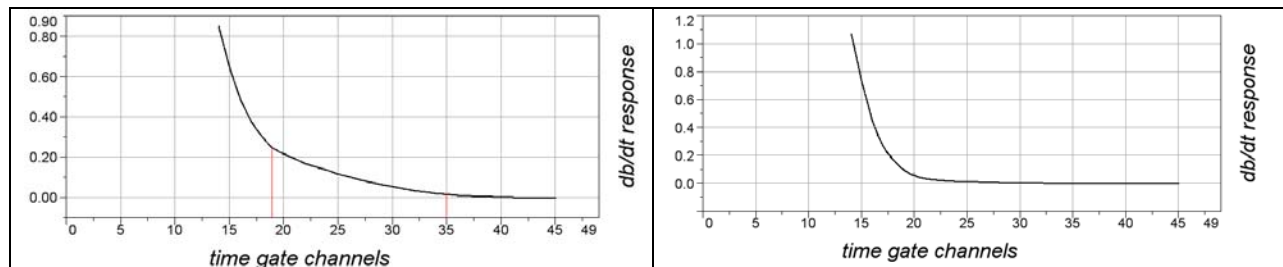
Figure E-1: Left – presence of good conductor, right – poor conductor.

---

[1] McNeill, JD, 1980, "Applications of Transient Electromagnetic Techniques", Technical Note TN-7 page 5, Geonics Limited, Mississauga, Ontario.

EM Time Constant (Tau) Calculation

The EM Time-Constant (TAU) is a general measure of the speed of decay of the electromagnetic response and indicates the presence of eddy currents in conductive sources as well as reflecting the "conductance quality" of a source. Although TAU can be calculated using either the measured dB/dt decay or the calculated B-field decay, dB/dt is commonly preferred due to better stability (S/N) relating to signal noise. Generally, TAU calculated on base of early time response reflects both near surface overburden and poor conductors whereas, in the late ranges of time, deep and more conductive sources, respectively. For example early time TAU distribution in an area that indicates conductive overburden is shown in Figure 2.
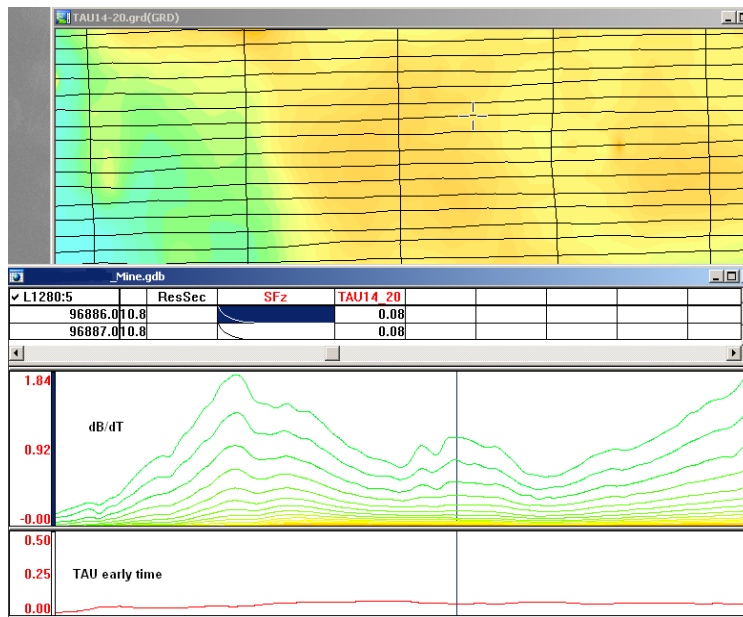
Figure E-2: Map of early time TAU. Area with overburden conductive layer and local sources.
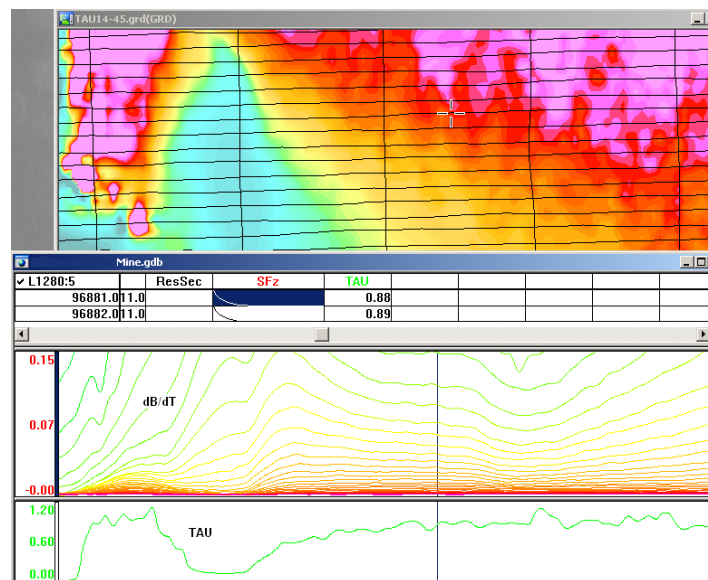
Figure E-3: Map of full time range TAU with EM anomaly due to deep highly conductive target.

There are many advantages of TAU maps:

- TAU depends only on one parameter (conductance) in contrast to response magnitude;
- TAU is integral parameter, which covers time range and all conductive zones and targets are displayed independently of their depth and conductivity on a single map.
- Very good differential resolution in complex conductive places with many sources with different conductivity.
- Signs of the presence of good conductive targets are amplified and emphasized independently of their depth and level of response accordingly.

In the example shown in Figure 4 and 5, three local targets are defined, each of them with a different depth of burial, as indicated on the resistivity depth image (RDI). All are very good conductors but the deeper target (number 2) has a relatively weak dB/dt signal yet also features the strongest total TAU (Figure 4). This example highlights the benefit of TAU analysis in terms of an additional target discrimination tool.
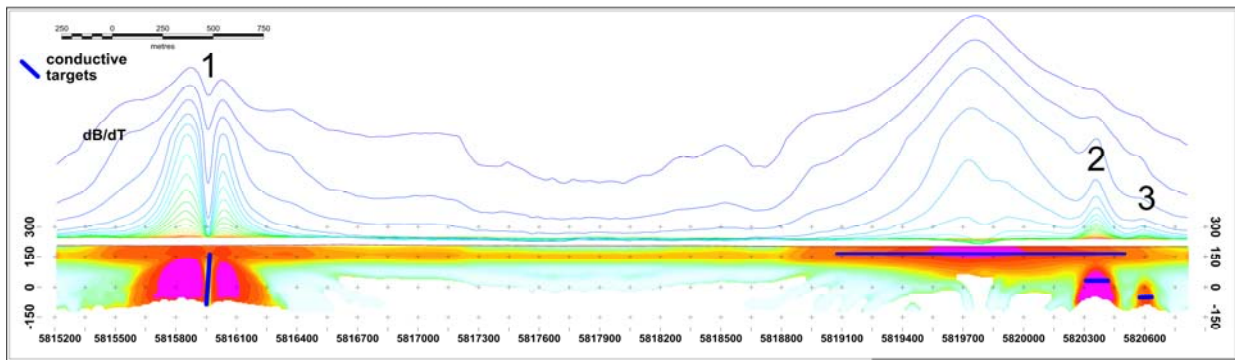
Figure E-4: dB/dt profile and RDI with different depths of targets.
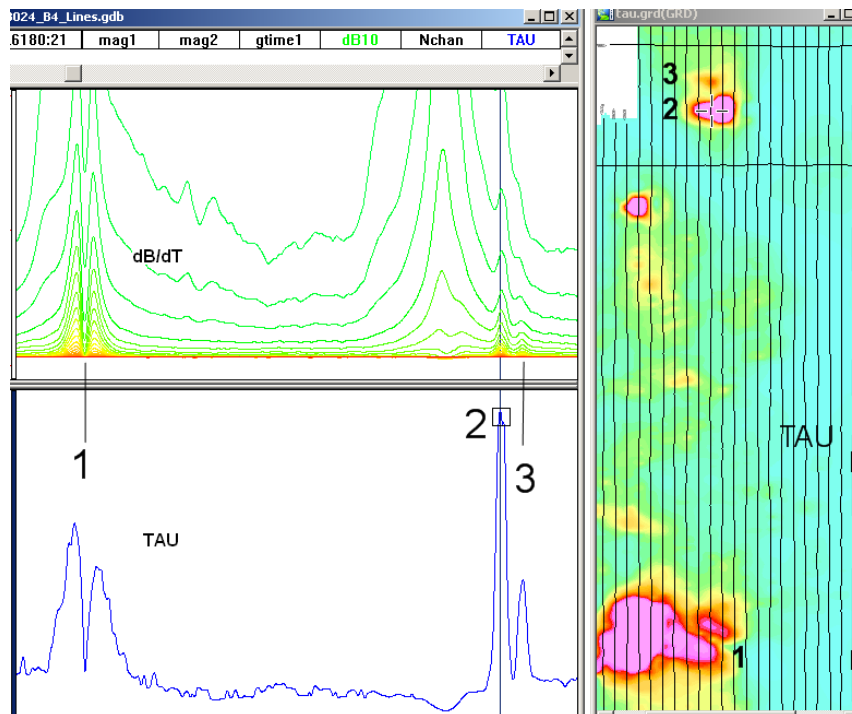
Figure E-5: Map of total TAU and dB/dt profile.

The EM Time Constants for dB/dt and B-field were calculated using the "sliding Tau" in-house program developed at Geotech[2]. The principle of the calculation is based on using of time window (4 time channels) which is sliding along the curve decay and looking for latest time channels which have a response above the level of noise and decay. The EM decays are obtained from all available decay channels, starting at the latest channel. Time constants are taken from a least square fit of a straight-line (log/linear space) over the last 4 gates above a pre-set signal threshold level (Figure F6). Threshold settings are pointed in the "label" property of TAU database channels. The sliding Tau method determines that, as the amplitudes increase, the time-constant is taken at progressively later times in the EM decay. Conversely, as the amplitudes decrease, Tau is taken at progressively earlier times in the decay. If the maximum signal amplitude falls below the threshold, or becomes negative for any of the 4 time gates, then Tau is not calculated and is assigned a value of "dummy" by default.
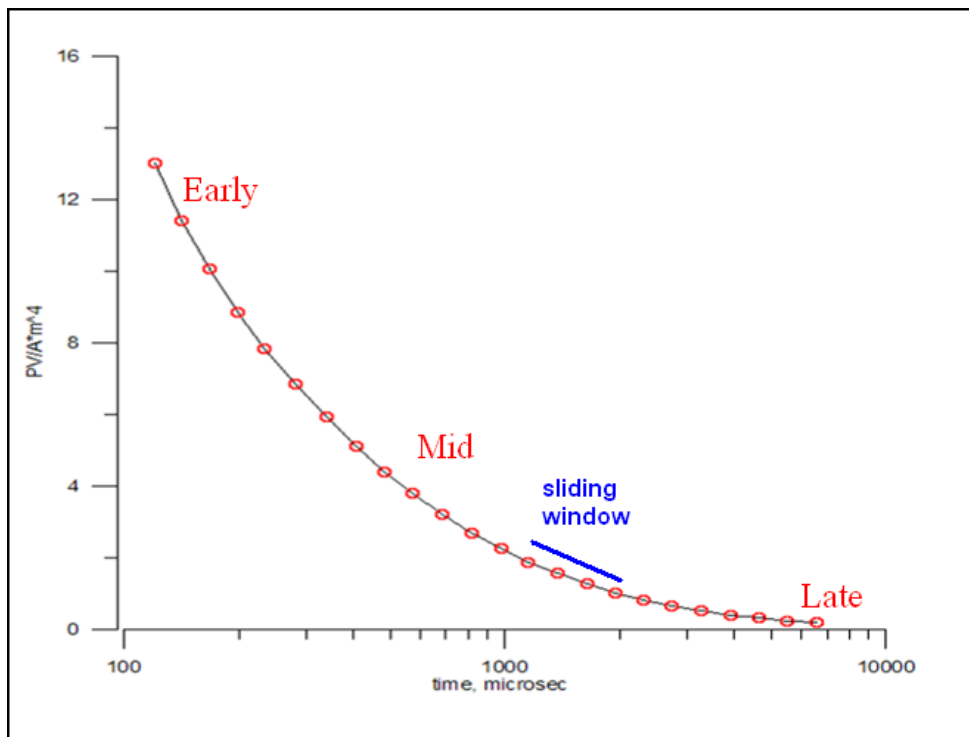
Figure E-6: Typical dB/dt decays of Vtem data

Alexander Prikhodko, PhD, P.Geo
Geotech Ltd.

September 2010

---

[2] by A.Prikhodko

APPENDIX F

TEM RESISTIVITY DEPTH IMAGING (RDI)

Resistivity depth imaging (RDI) is technique used to rapidly convert EM profile decay data into an equivalent resistivity versus depth cross-section, by deconvolving the measured TEM data.
The used RDI algorithm of Resistivity-Depth transformation is based on scheme of the apparent resistivity transform of Maxwell A.Meju (1998)[1] and TEM response from conductive half-space. The program is developed by Alexander Prikhodko and depth calibrated based on forward plate modeling for VTEM system configuration (Fig. 1-10).

RDIs provide reasonable indications of conductor relative depth and vertical extent, as well as accurate 1D layered-earth apparent conductivity/resistivity structure across VTEM flight lines. Approximate depth of investigation of a TEM system, image of secondary field distribution in half space, effective resistivity, initial geometry and position of conductive targets is the information obtained on base of the RDIs.

Maxwell forward modeling with RDI sections from the synthetic responses (VTEM system)
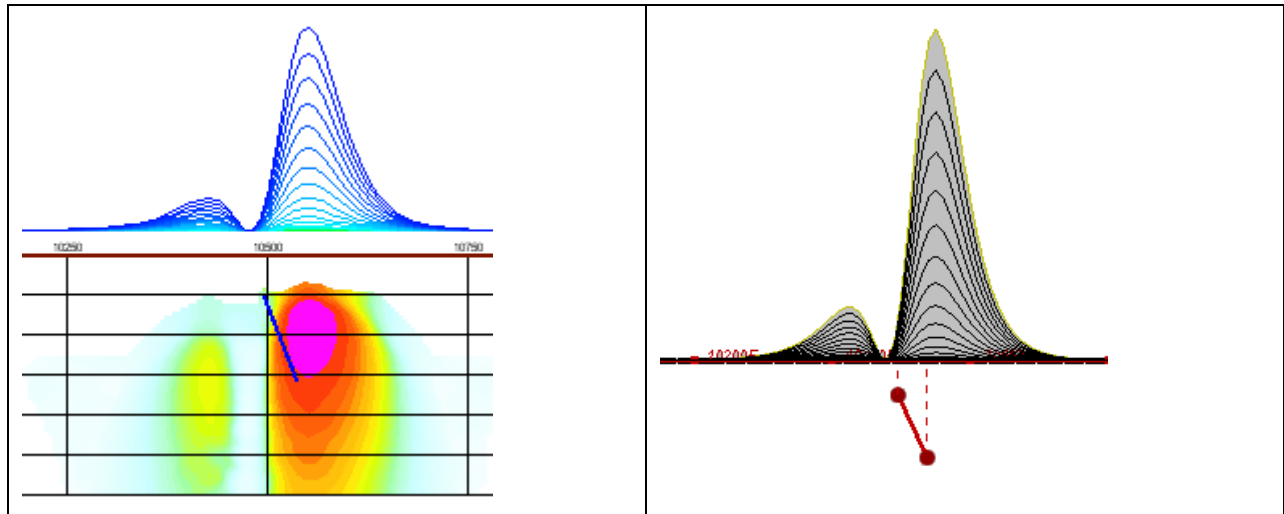
Figure F-1: Maxwell plate model and RDI from the calculated response for conductive "thin" plate (depth 50 m, dip 65 degree, depth extend 100 m).

---

[1] Maxwell A.Meju, 1998, Short Note: A simple method of transient electromagnetic data analysis, Geophysics, **63**, 405–410.
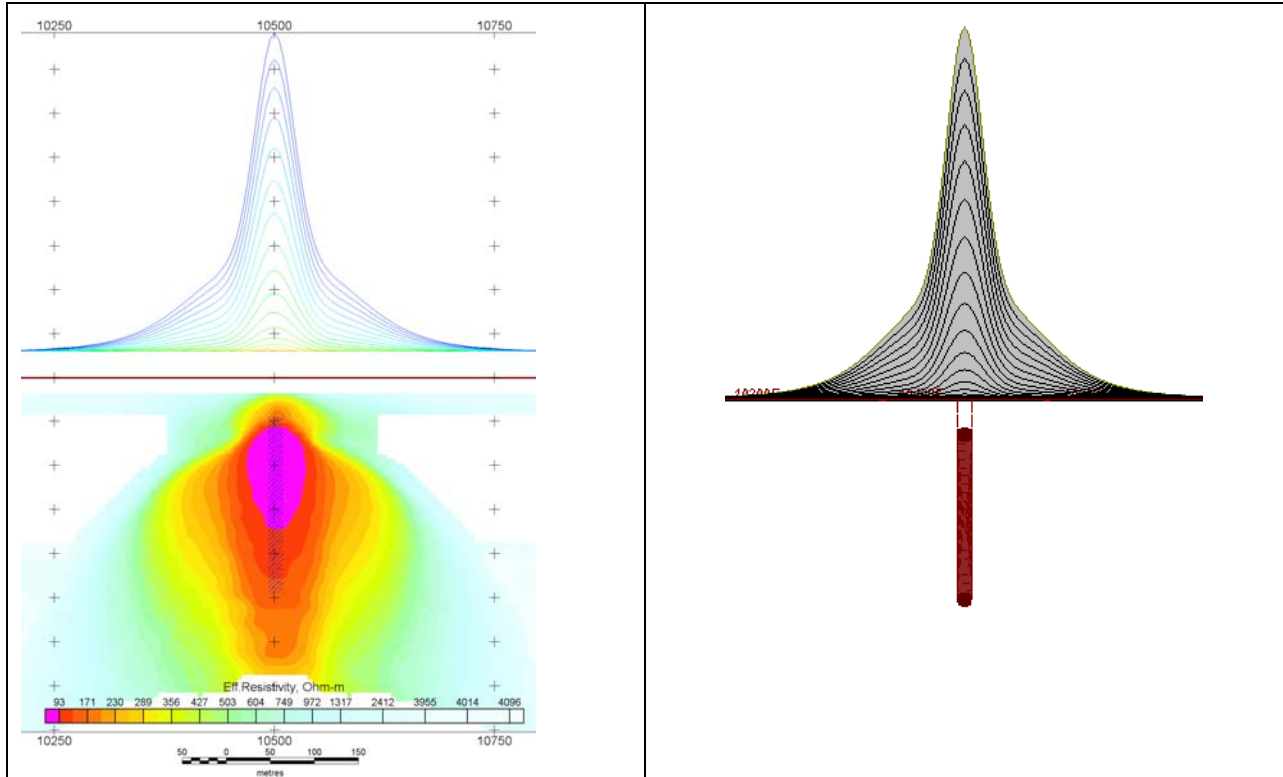
Figure F-2: Maxwell plate model and RDI from the calculated response for "thick" plate 18 m thickness, depth 50 m, depth extend 200 m).
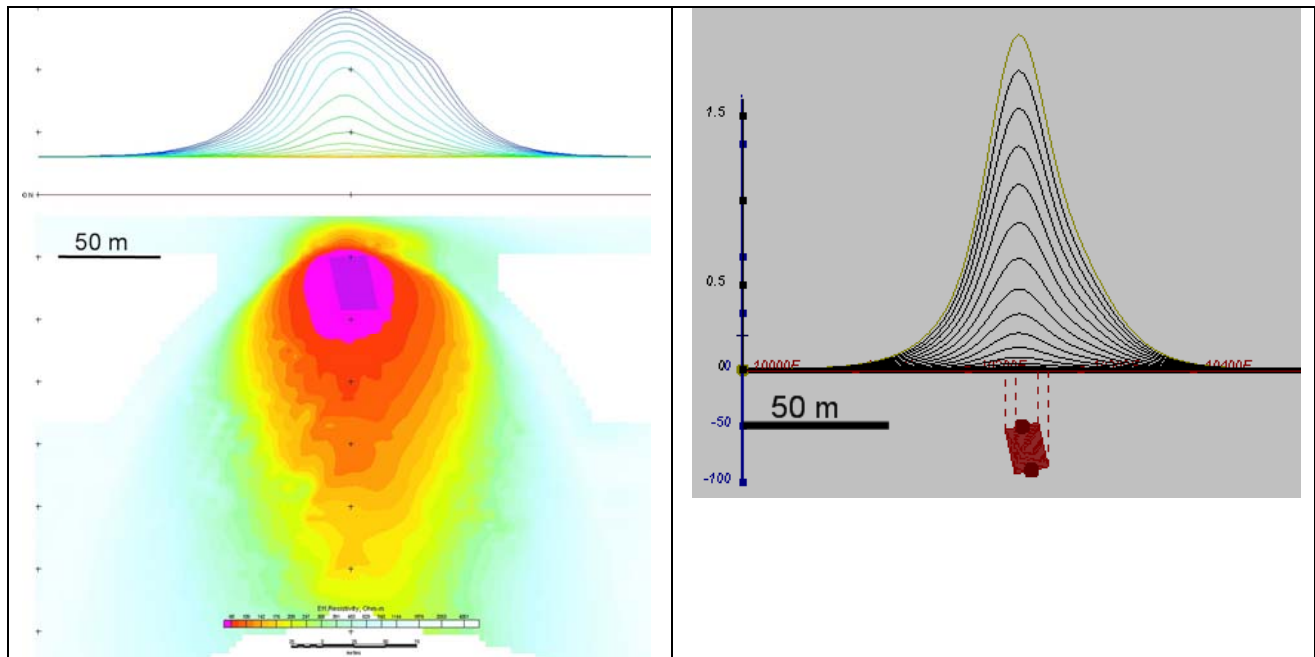
Figure F-3: Maxwell plate model and RDI from the calculated response for bulk ("thick") 100 m length, 40 m depth extend, 30 m thickness
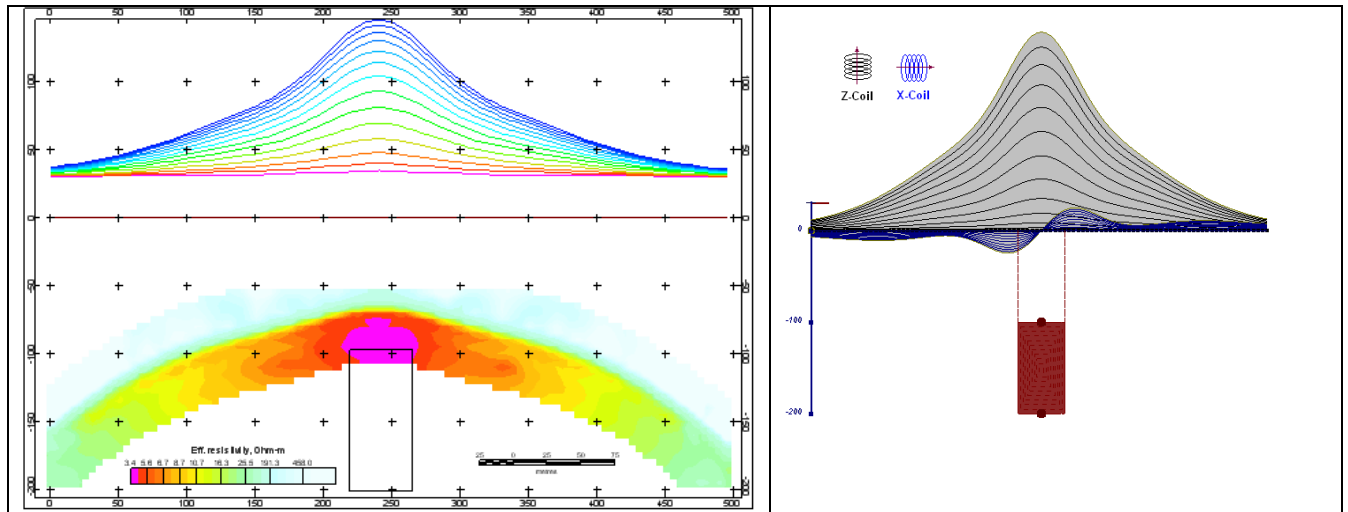
Figure F-4: Maxwell plate model and RDI from the calculated response for "thick" vertical target (depth 100 m, depth extend 100 m). 19-44 chan.
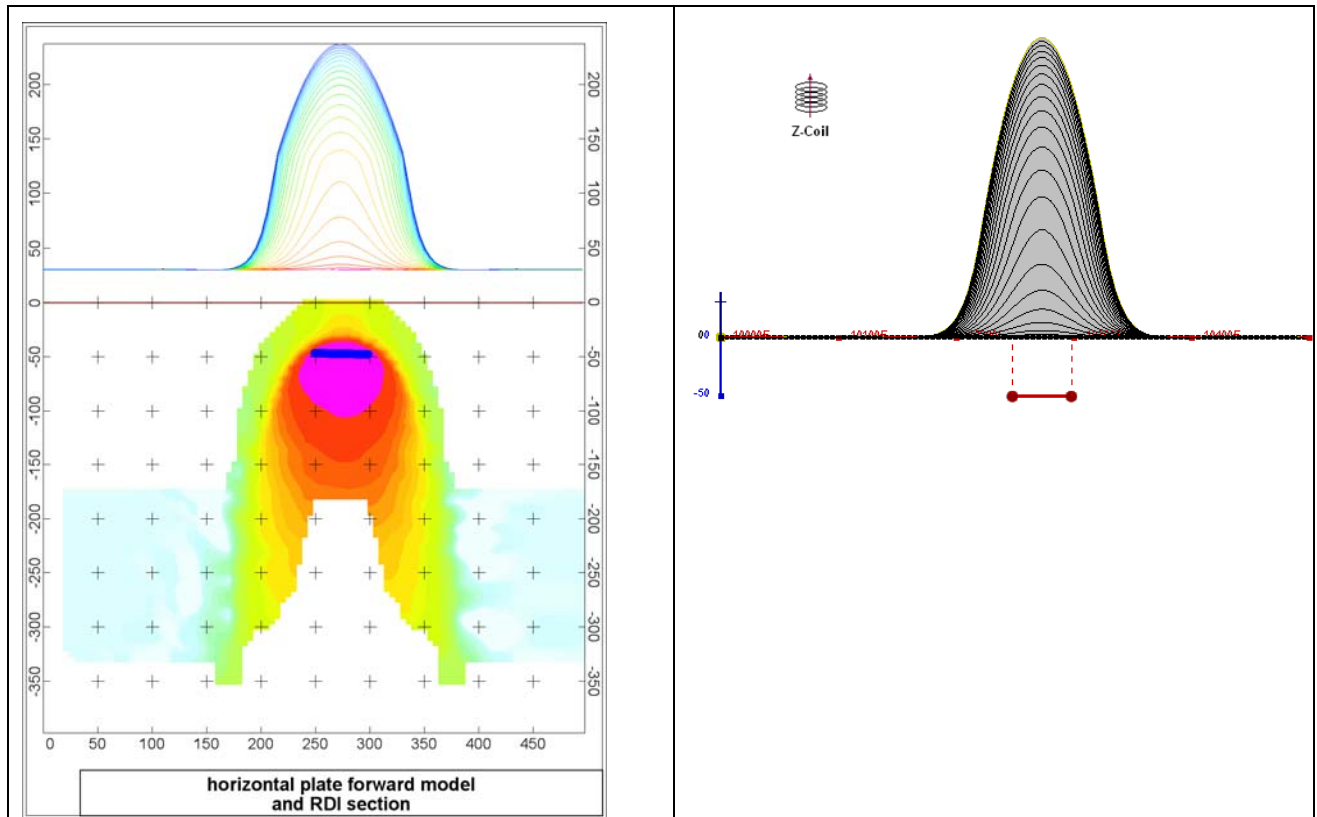

Figure F-5: Maxwell plate model and RDI from the calculated response for horizontal thin plate (depth 50 m, dim 50x100 m). 15-44 chan.
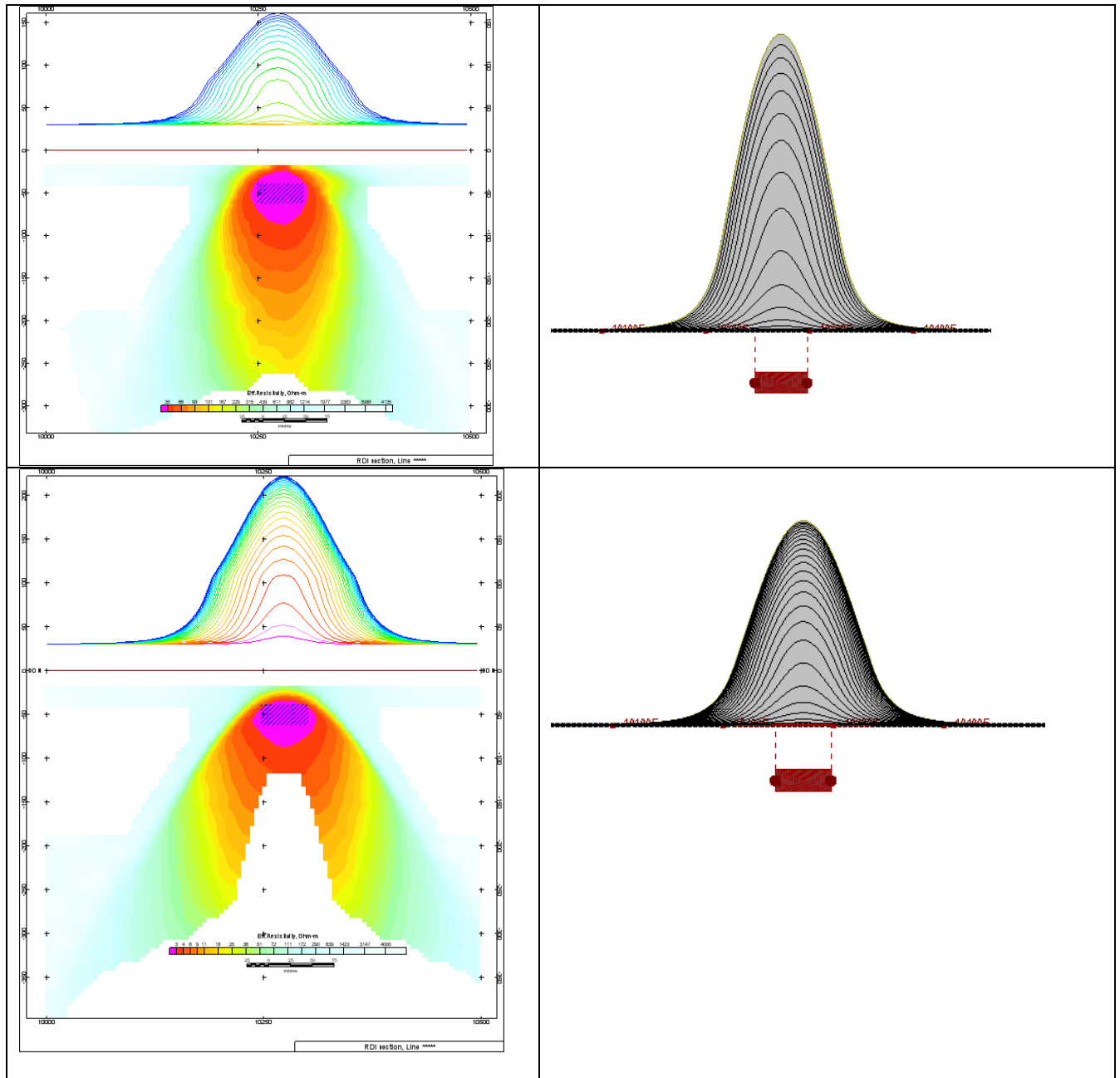
Figure F-6: Maxwell plate model and RDI from the calculated response for horizontal thick (20m) plate – less conductive (on the top), more conductive (below)
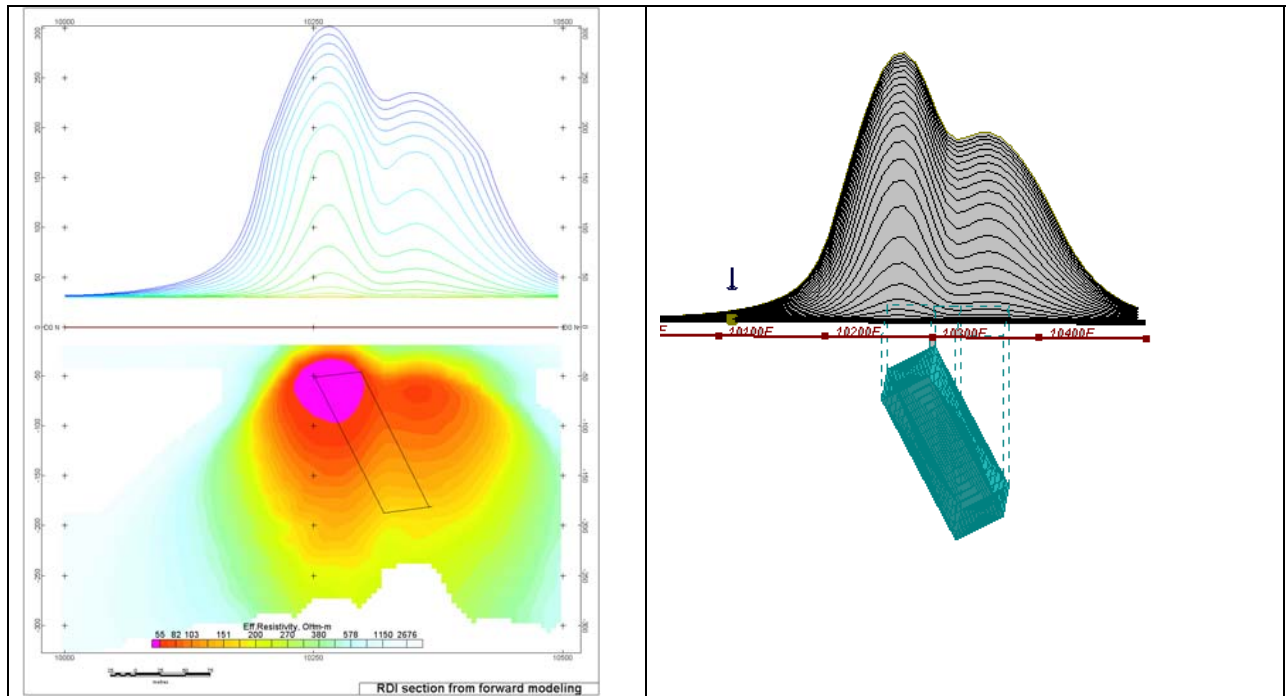
Figure F-7: Maxwell plate model and RDI from the calculated response for inclined thick (50m) plate. Depth extends 150 m, depth to the target 50 m.
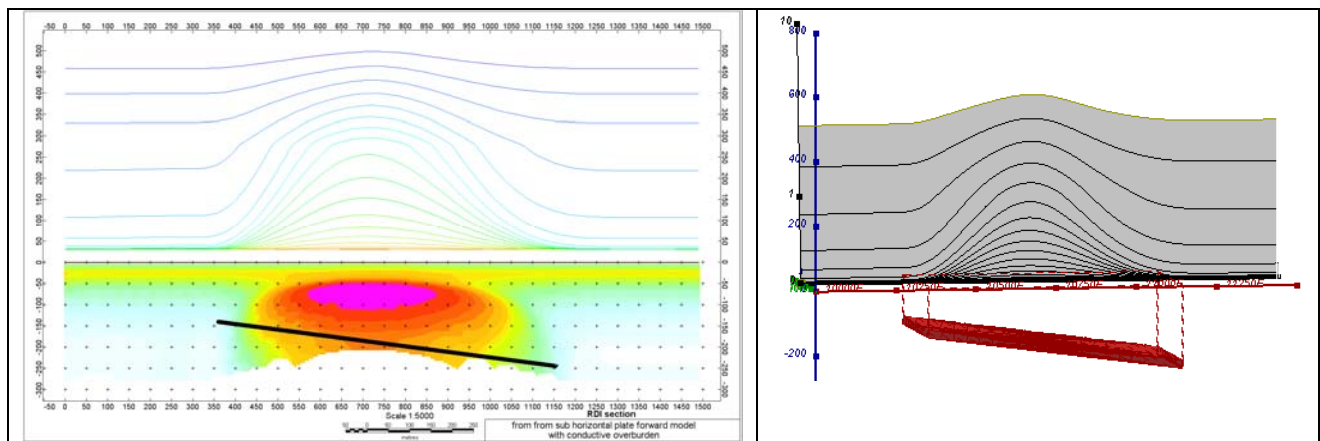
Figure F-8: Maxwell plate model and RDI from the calculated response for the long, wide and deep subhorizontal plate (depth 140 m, dim 25x500x800 m) with conductive overburden.
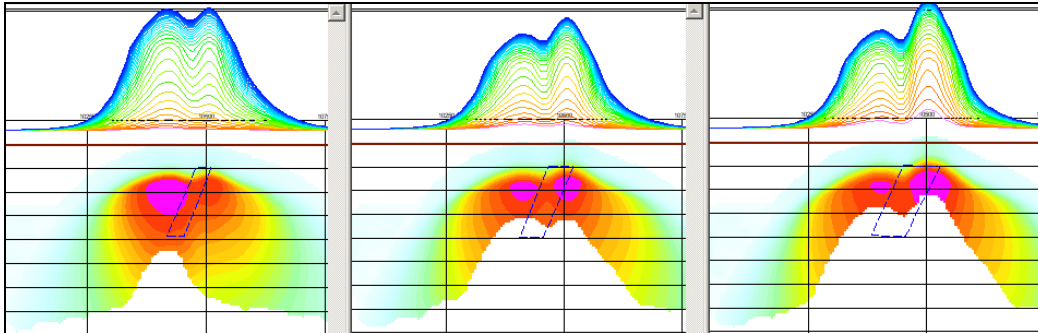
Figure F-9: Maxwell plate models and RDIs from the calculated response for "thick" dipping plates (35, 50, 75 m thickness), depth 50 m, conductivity 2.5 S/m.
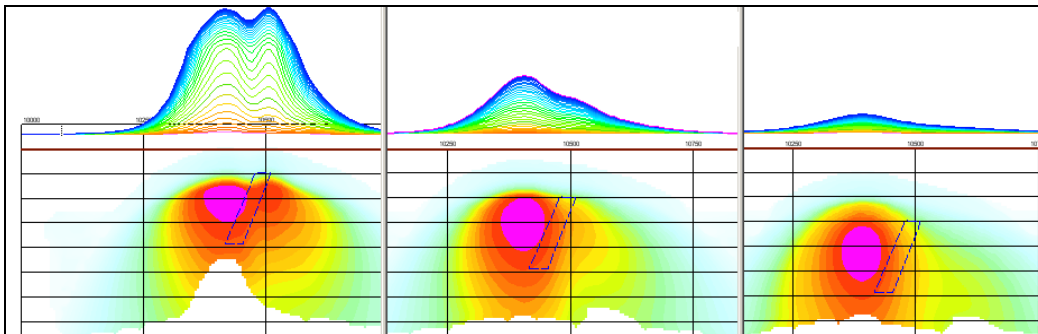
Figure F-10: Maxwell plate models and RDIs from the calculated response for "thick" (35 m thickness) dipping plate on different depth (50, 100, 150 m),, conductivity 2.5 S/m.
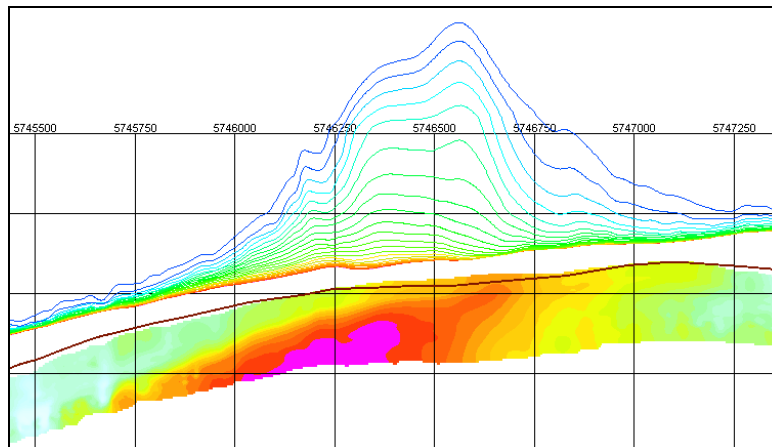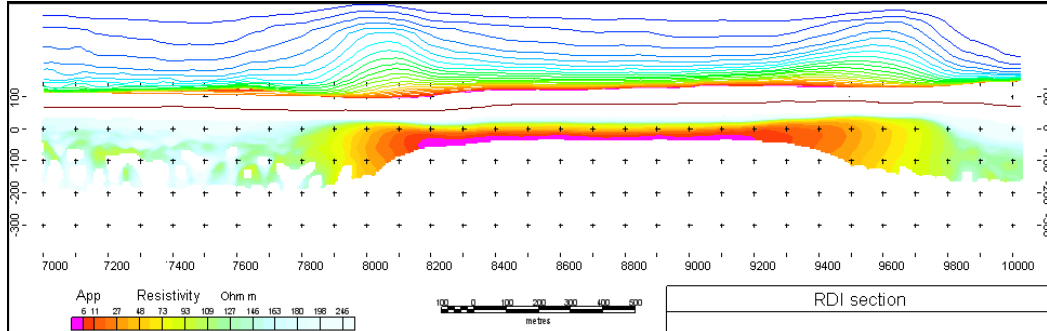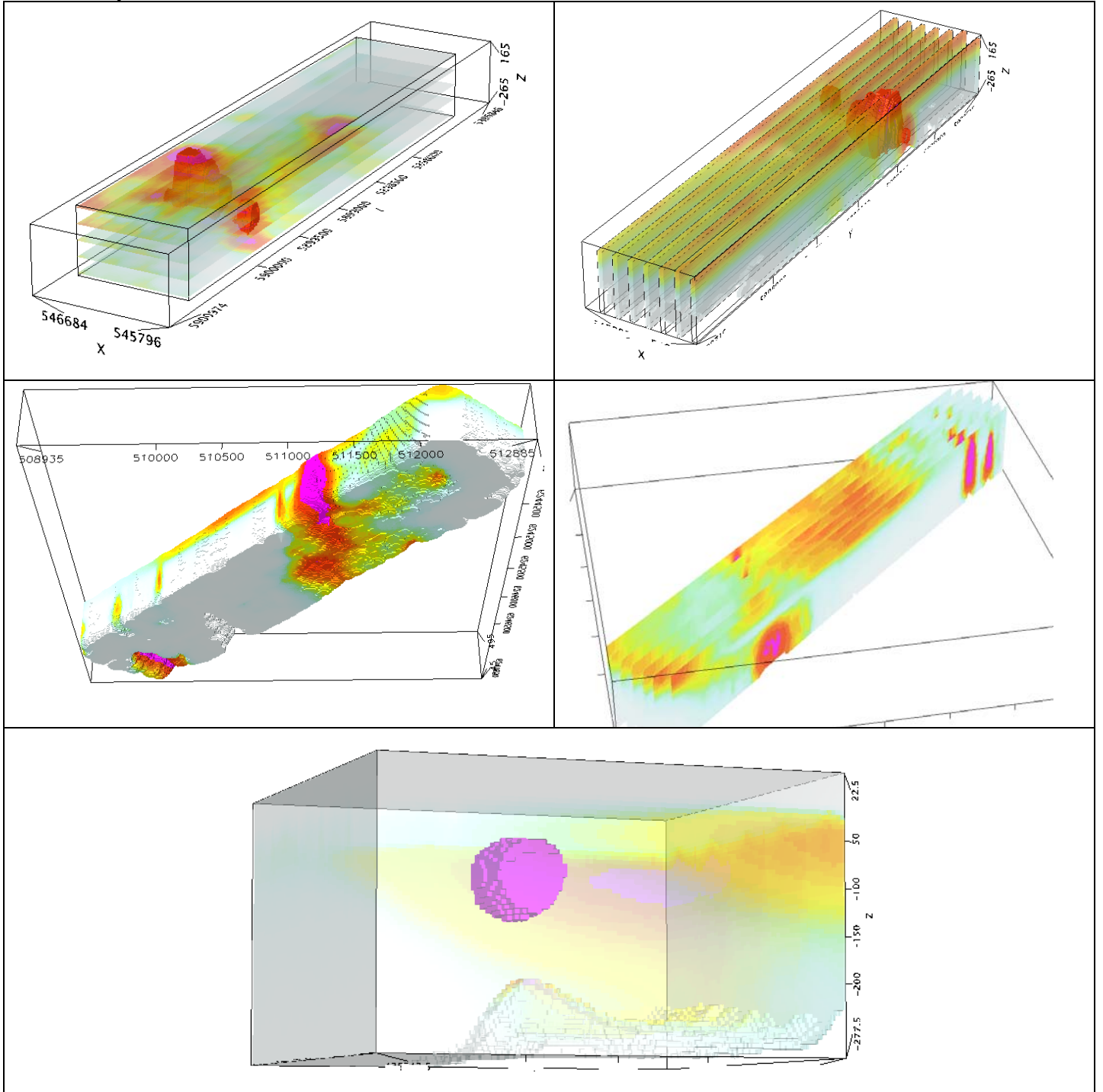

Figure F-11: RDI section for the real horizontal and slightly dipping conductive layers

FORMS OF RDI PRESENTATION

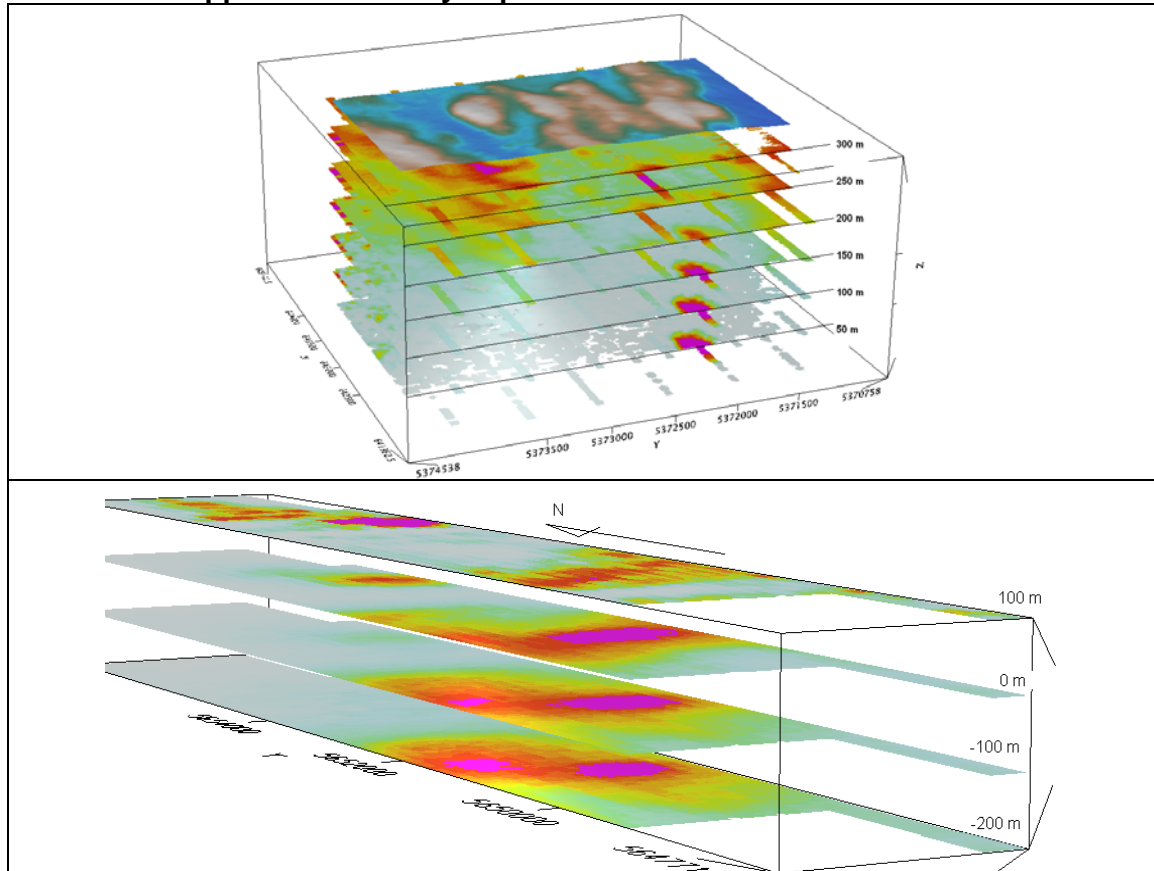## Presentation of series of lines

Scale 1:10000

Vertical Exaggeration: 1

SECTION PLOT
rdi

Geotech Ltd.
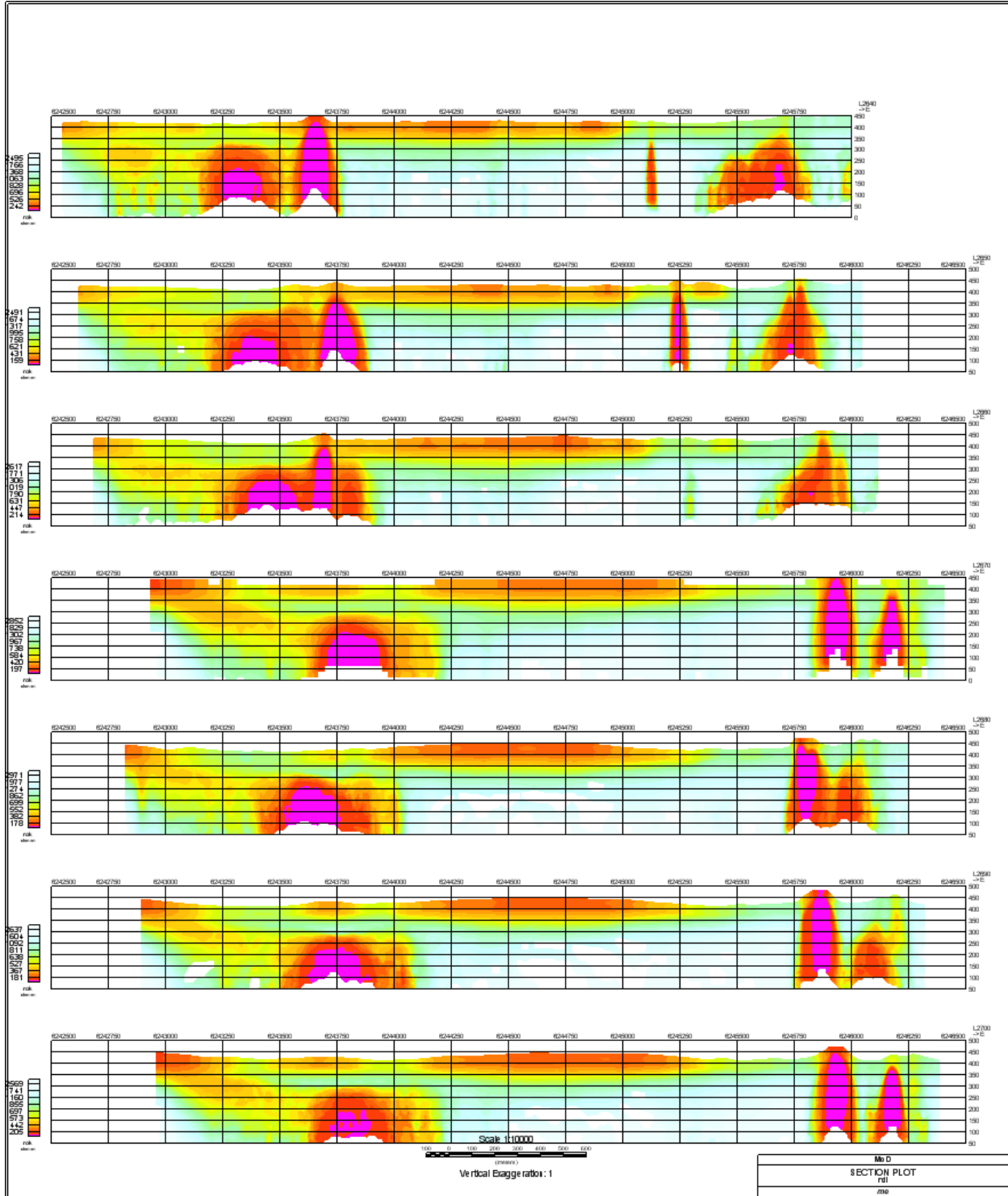
3d presentation of RDIs

Apparent Resistivity Depth Slices plans:
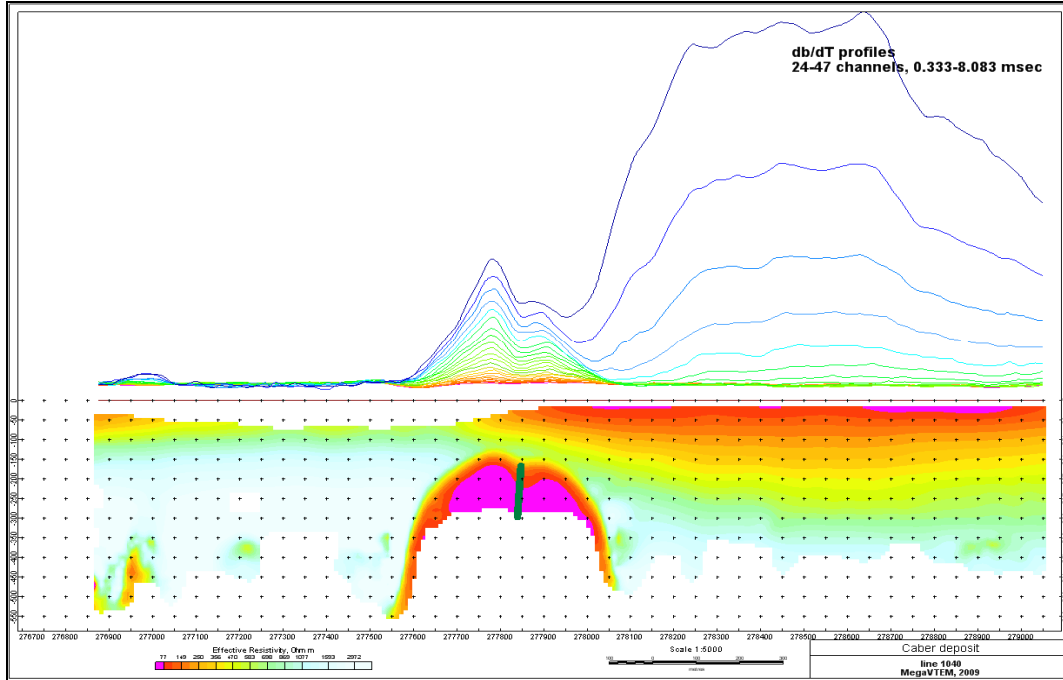

| 0 m (surface) | -100 m | -200 m |
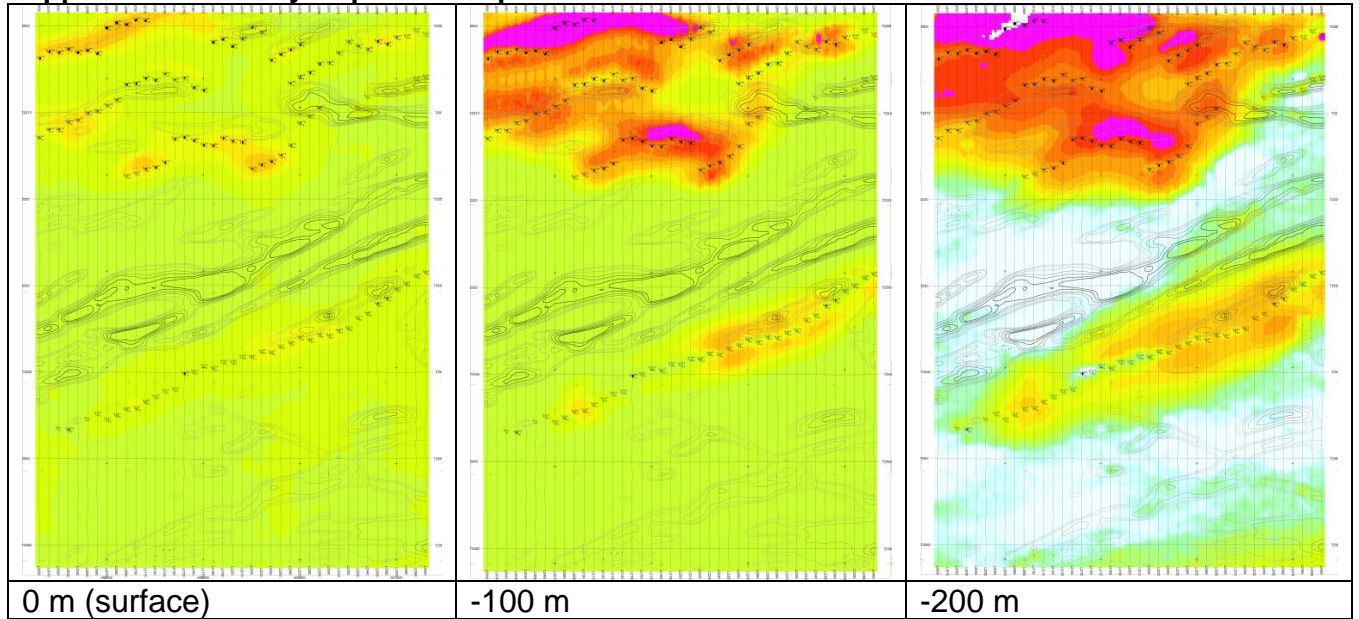
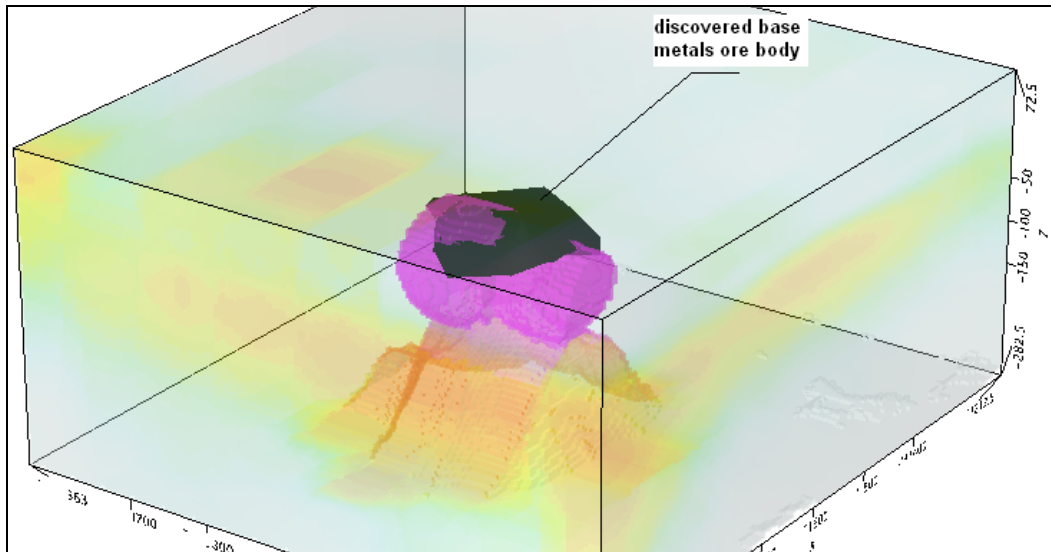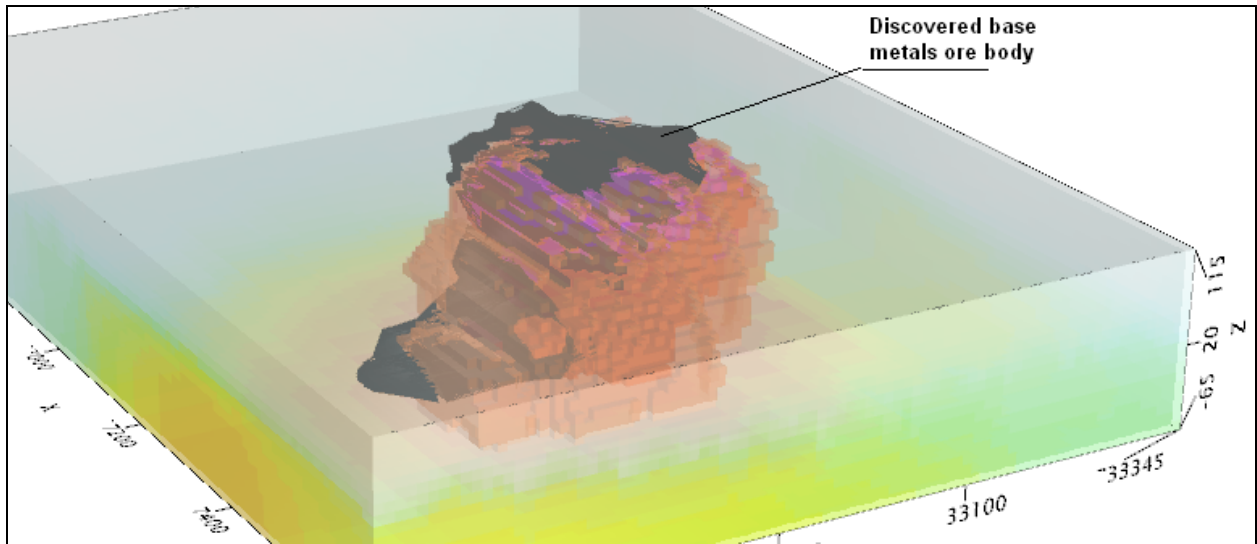**3d views of apparent resistivity depth slices:**

Real base metal targets in comparison with RDIs:

RDI section of the line over Caber deposit ("thin" subvertical plate target and conductive overburden).

3d RDI voxels with base metals ore bodies (Middle East):

Discovered base metals ore body

Alexander Prikhodko, PhD, P.Geo
Geotech Ltd.
April 2011